Biogeosciences, 15, 669–691, 2018
https://doi.org/10.5194/bg-15-669-2018

Biogeosciences Open Access EGU

Hydro-ecological controls on dissolved carbon dynamics in groundwater and export to streams in a temperate pine forest

Loris Deirmendjian[1], Denis Loustau[2], Laurent Augusto[2], Sébastien Lafont[2], Christophe Chipeaux[2], Dominique Poirier[1], and Gwenaël Abril[1,3,a]

[1]Laboratoire Environnements et Paléoenvironnements Océaniques et Continentaux (EPOC), CNRS, Université de Bordeaux, Allée Geoffroy Saint-Hilaire, 33615 Pessac CEDEX, France
[2]INRA, UMR 1391 Interactions Sol-Plante-Atmosphère (ISPA), 33140 Villenave-d'Ornon, France
[3]Departamento de Geoquímica, Universidade Federal Fluminense, Outeiro São João Batista s/n, 24020015, Niterói, RJ, Brazil
[a]also at: Laboratoire d'Océanographie et du Climat, Expérimentations et Approches Numériques (LOCEAN), Centre IRD France-Nord, 32, Avenue Henri Varagnat, 93143 Bondy, France

Correspondence: Loris Deirmendjian (lorisdeir@gmail.com)

Received: 14 March 2017 – Discussion started: 12 April 2017
Revised: 10 December 2017 – Accepted: 28 December 2017 – Published: 1 February 2018

Abstract. We studied the export of dissolved inorganic carbon (DIC) and dissolved organic carbon (DOC) from forested shallow groundwater to first-order streams, based on groundwater and surface water sampling and hydrological data. The selected watershed was particularly convenient for such study, with a very low slope, with pine forest growing on sandy permeable podzol and with hydrology occurring exclusively through drainage of shallow groundwater (no surface runoff). A forest plot was instrumented for continuous eddy covariance measurements of precipitation, evapotranspiration, and net ecosystem exchanges of sensible and latent heat fluxes as well as CO_2 fluxes. Shallow groundwater was sampled with three piezometers located in different plots, and surface waters were sampled in six first-order streams; river discharge and drainage were modeled based on four gauging stations. On a monthly basis and on the plot scale, we found a good consistency between precipitation on the one hand and the sum of evapotranspiration, shallow groundwater storage and drainage on the other hand. DOC and DIC stocks in groundwater and exports to first-order streams varied drastically during the hydrological cycle, in relation with water table depth and amplitude. In the groundwater, DOC concentrations were maximal in winter when the water table reached the superficial organic-rich layer of the soil. In contrast, DIC (in majority excess CO_2) in groundwater showed maximum concentrations at low water table during late summer, concomitant with heterotrophic conditions of the forest plot. Our data also suggest that a large part of the DOC mobilized at high water table was mineralized to DIC during the following months within the groundwater itself. In first-order streams, DOC and DIC followed an opposed seasonal trend similar to groundwater but with lower concentrations. On an annual basis, leaching of carbon to streams occurred as DIC and DOC in similar proportion, but DOC export occurred in majority during short periods of the highest water table, whereas DIC export was more constant throughout the year. Leaching of forest carbon to first-order streams represented a small portion (approximately 2 %) of the net land CO_2 sink at the plot. In addition, approximately 75 % of the DIC exported from groundwater was not found in streams, as it returned very fast to the atmosphere through CO_2 degassing.

1 Introduction

Since the beginning of the industrial era, human activities have greatly modified the fluxes of carbon between the atmosphere and the continents, as well as those occurring along the aquatic continuum that connect land and the coastal ocean (Ciais et al., 2013; Cole et al., 2007; Regnier et al., 2013). Globally, land (vegetation and soil) is a major reservoir of carbon that acts as a net annual sink of atmospheric CO_2, therefore modulating the climate system (Ciais et al.,

2013; Heimann and Reichstein, 2008), and is thought to offer a mitigation strategy to reduce global warming (Schimel et al., 2001). In European forests, 70 % of the net land sink is sequestered in plants as woody biomass increments and 30 % is sequestered in soils (Luyssaert et al., 2010). However, large uncertainty concerning the drivers and future of the soil organic carbon remains (Luyssaert et al., 2010). Therefore, investigating the mechanisms that impact storage and export of soil carbon from forest ecosystems is of first interest in both ecosystem and climate research.

Streams and small rivers are important links between terrestrial and aquatic ecosystems because they receive inputs of carbon from land and then transform these materials at the land–stream interface and in stream channels as water flows to larger rivers (McClain et al., 2003; Raymond et al., 2013). The carbon dynamics in forest stream ecosystems results from the interaction among biological activity, weathering, water infiltration, drainage and retention–mobilization mechanisms in soils (Jones and Mulholland, 1998; Kawasaki et al., 2005; Shibata et al., 2001). Indeed, biogeochemical cycling within and across the terrestrial–aquatic interface is dynamically linked to the water cycle (Battin et al., 2009; Johnson et al., 2006) because dissolved carbon is primarily mobilized and transported by the movement of water (Hagerdon et al., 2000; Hope et al., 1994; Kawasaki et al., 2005). Furthermore, numerous works in different environments came to the same conclusion that streams and small rivers are hotspots of CO_2 degassing (Butman and Raymond, 2011; Johnson et al., 2008; Kokic et al., 2015; Polsenaere and Abril, 2012; Wallin et al., 2013). In small streams, the CO_2 degassing flux primary results from inputs of groundwater enriched in CO_2 (Hotchkiss et al., 2015), which comes from plant root respiration and from microbial respiration in soils and groundwater.

The quantification of dissolved carbon fluxes transported by water from terrestrial to aquatic environments is fundamental to resolving the carbon balance on the catchment scale (Billett et al., 2004; Jonsson et al., 2007; Kindler et al., 2011; Magin et al., 2017; Shibata et al., 2005). Leaching of carbon from terrestrial ecosystems to streams could potentially represent up to 160 % of the net ecosystem exchange (NEE) in a Scotland peat catchment (Billett et al., 2004), 6 % in a Sweden boreal catchment dominated by coniferous forest (Jonsson et al., 2007), on average 6 % in five forest plots across Europe (Kindler et al., 2011), 2 % in a Japanese temperate catchment dominated by deciduous forest (Shibata et al., 2005) or 2.7 % of the net primary production in different woody and tilled subcatchments across southwestern Germany (Magin et al., 2017). Such large variations in carbon export rates are not well understood and it is therefore important to extend this investigation to other landscapes and climatic zones. More studies focused on the processes that govern the mobilization of soil carbon to surface waters are necessary to improve and predict carbon budgets in terrestrial ecosystems.

Some authors reported high concentrations of dissolved inorganic carbon (DIC) (Kawasaki et al., 2005; Venkiteswaran et al., 2014) and dissolved organic carbon (DOC) (Artinger et al., 2000; Baker et al., 2000) in forest-dominated groundwater (i.e., in the saturated zone of the soil). However, estimations of terrestrial carbon leaching from direct simultaneous measurements in groundwater and streams are scarce. These studies are generally restricted to submarine and coastal environments (Atkins et al., 2013; Sadat-Noori et al., 2016; Santos et al., 2012) and boreal lakes (Einarsdottir et al., 2017), but rarely streams. The few studies that estimate exports of carbon from forested landscapes to streams are generally (i) based on carbon observations in soil water (i.e., in the unsaturated zone of the soil) combined with a soil water model that simulates the volume of soil water leached to streams (Öquist et al., 2009; Kindler et al., 2011; Leith et al., 2015), (ii) based on carbon observations in stream combined with stream discharge (Billett et al., 2004; Dawson et al., 2002; Olefeldt et al., 2013; Shibata et al., 2001, 2005), or (iii) as described by the active pipe concept (Cole et al., 2007), as the sum of the three major riverine carbon fluxes: CO_2 degassing, organic carbon burial in sediments and carbon export downstream (Jonsson et al., 2007). These studies do not provide a complete understanding of the link between carbon hydrological export and the physicochemical and biological processes occurring in soils and groundwater. In addition, the approaches based on only stream sampling may miss part of the DIC export flux as excess CO_2 that might rapidly degas upstream of the sampling points (Venkiteswaran et al., 2014).

In this study, we instrumented a temperate watershed that offers the convenience of a homogeneous lithology (permeable sandy soil), vegetation (pine forest), topography (very flat coastal plain), and a simple hydrology functioning exclusively as shallow groundwater drainage. This simple configuration with no surface runoff allows us to identify what are the main factors that control the DIC–DOC leaching to streams, the DIC : DOC ratio in groundwater and streams, and their variation in space and over time. On the plot scale, we relate DIC and DOC temporal dynamics in groundwater with hydrology and metabolic activity of the forest ecosystem. On the watershed scale, we quantify DIC and DOC transfers through the groundwater–stream interface, and we describe the fate of this carbon in first-order streams.

2 Materials and methods

2.1 Study site

The Leyre watershed (2100 km^2) is located in the southwest of France, in the "Landes de Gascogne" area (Fig. 1). The landscape is a very flat coastal plain with a mean slope lower than 0.125 % (generally NW–SE) (Jolivet et al., 2007), but with local gentle slopes (notably near some streams). The

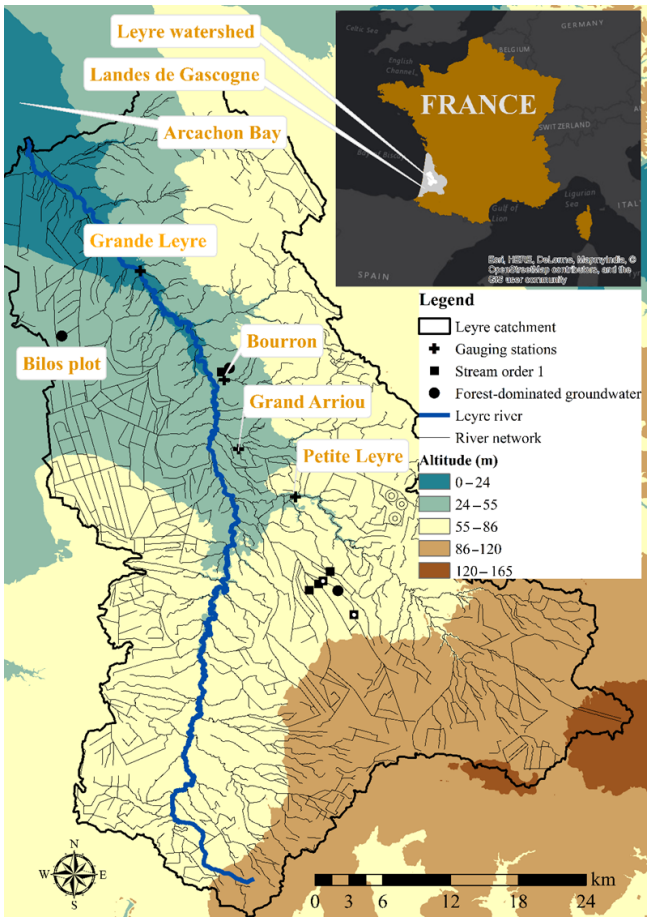

Figure 1. Map of the Leyre watershed with topography showing the location of the gauging stations (the Grande Leyre, the Petite Leyre, the Grand Arriou and the Bourron rivers), the Bilos site, and the other sampled piezometers and first-order streams. The rain gauge and eddy tower are located at the Bilos plot. White circles indicate the first-order streams where additional discharge measurements were made in April 2014 and February 2015.

mean altitude is lower than 50 m (Fig. 1) (Jolivet et al., 2007). The lithology is relatively homogeneous and composed of sandy permeable surface layers dating from the Pliocene–Quaternary period (Bertran et al., 2009, 2011; Legigan, 1979).

The podzolic soil is characterized by a low pH (4), low nutrient availability, and a high organic carbon content that can reach 55 g kg^{-1} of soil (Augusto et al., 2010). Three types of podzols are present: wet Landes (humic podzol), mesophyllous Landes (duric podzol) and dry Landes (loose podzol), which represent 47, 36 and 17 % of the watershed area, respectively (Augusto et al., 2010; Jolivet et al., 2007). Moreover, there is a gradient of soil carbon content from dry Landes ($C = 6$ to 17 kg m^{-2}) to mesophyllous Landes ($C = 13$ to 30 kg m^{-2}) and wet Landes ($C = 15$ to 30 kg m^{-2}) (Augusto et al., 2010). In the dry Landes of the upper parts of the watershed, the water table is always more than 2 m deep. In the wet Landes of the lower parts, and in the vast interfluves, the groundwater is found near the soil surface in winter (0.0–0.5 m depth) and generally remains 1.0–1.5 m deep in summer. The mesophyllous Landes corresponds to the intermediate situation (Augusto et al., 2006).

The region was a vast wetland until the 19th century, when a wide forest of maritime pine (*Pinus pinaster*) was sown, following landscape drainage in 1850. Currently, the catchment is mainly occupied by pine forest (approximately 80 %), with a modest proportion of croplands (approximately 15 %) (Jolivet et al., 2007). The typical rotation period of pine forest is ∼ 40 years, ending in clear-cutting, tilling and replanting (Kowalski et al., 2003). The climate is oceanic with a mean annual air temperature of 13 °C and a mean annual precipitation of 930 mm (Moreaux et al., 2011). Moreover, the average annual evapotranspiration of maritime pine is in the range of 234–570 mm (Govind et al., 2012). Owing to the low slope and the high permeability of the soil (hydraulic conductivity is approximately 40 cm h^{-1}; Corbier et al., 2010), the infiltration of rain water is fast (55 cm h^{-1} on average; Vernier and Castro, 2010) and surface runoff does not occur, as the excess rainfall percolates into the soil and recharges the shallow groundwater, causing the water table to rise. Moreover, very low content in feldspars and all over clay minerals in the sandy podzols induces a low water soil retention (Augusto et al., 2010). The superficial sandy soil contains a free and continuous water table strongly interconnected with the superficial river network; drainage is also facilitated by a dense network of drainage ditches built in the 19th century and currently maintained by forest managers in order to optimize tree growth (Thivolle-Cazat and Najar, 2001). In this study, we sampled first-order streams defined as streams and ditches with no tributaries and/or being seasonally dry.

2.2 Eddy covariance measurements on the forest plot scale

To quantify exchanges of carbon and water between the atmosphere and the pine forest plot, we used the site of Bilos (Fig. 1) (0.6 km^2, 44°29′38.08″ N, 0°57′21.9″ W, altitude: 40 m) as part of the ICOS research infrastructure (http://icos-ri.eu). In December 1999, the 50-year-old pine forest was clear-cut (Kowalski et al., 2003). The site was ploughed to 30 cm depth and fertilized with 60 kg of P_2O_5 per ha in 2001 (Moreaux et al., 2011). In November 2004, the site was divided into two parts, which were seeded with maritime pine (*Pinus pinaster*) with a 1-year lag in 2004 and 2005 (Moreaux et al., 2011). The forest plot was thus 10 and 11 years old during our sampling. The site was equipped with an eddy covariance measurement system soon after clear-cutting, and the system has been maintained since. The eddy covariance technique allows us to continuously determine the exchange of sensible heat, CO_2 and H_2O between the ecosystem and the atmosphere by measuring the turbulent-scale covariance

between vertical wind velocity and the scalar concentration of sensible heat, CO_2 and H_2O.

Wind velocity, temperature and CO_2–water vapor fluctuations were measured with a sonic anemometer (model R3, Gill instruments Lymington, UK) and an open-path dual CO_2–H_2O infrared gas analyzer (model Li7500, LI-COR, Lincoln, USA) at the top of a 9.6 m tower (1 January to 10 May 2014) and with another sonic anemometer (model HS50, Gill instruments) and an enclosed dual CO_2–H_2O infrared gas analyzer (model Li7200, LI-COR©) at the top of a 15 m tower (9 July 2014 to 31 December 2015). Consequently, there were no eddy covariance measurements available between 11 May and 8 July 2014 and thus between these two dates the latent heat fluxes were determined following the procedure of Thornthwaite (1948).

Raw data were processed following a standard methodology (Aubinet et al., 1999). The post-processing software EddyPro v6.0 (http://www.licor.com) was used to treat raw data and compute average fluxes (30 min period) by applying the following steps: (1) spike removal in anemometer or gas analyzer data using statistical analysis; (2) coordinating rotation to align the coordinate system with the stream lines of the 30 min averages; (3) blocking average detrending of sonic temperature, H_2O and CO_2 channels; (4) determining time lag values for H_2O and CO_2 channels using a cross-correlation procedure; (5) computing mean values, turbulent fluxes and characteristic parameters; and (6) making spectral corrections (Ibrom et al., 2007). Thereafter, CO_2 and H_2O fluxes were filtered in order to remove points corresponding to technical problems, meteorological conditions not satisfying eddy correlation theory or data out of realistic bounds. Different statistical tests were applied for this filtering: stationarity and turbulent conditions were tested with the steady-state test and the turbulence characteristic test recommended by Foken and Wichura (1996) and Kaimal and Finnigan (1994). Only values of CO_2 and H_2O fluxes that pass all the filters were retained. Then, missing values of CO_2 and H_2O fluxes were gap-filled. The NEE of CO_2 was partitioned into two components, gross primary production (GPP) and ecosystem respiration (R_{eco}), with the R package REddyProc (version 0.8-2) by applying the following steps (Reichstein et al., 2005).

(i) During nighttime GPP = 0 so NEE = R_{eco}. (ii) Statistical regression between R_{eco} and nighttime air temperature and meteorological conditions is adjusted with a Arrhenius-type equation (Lloyd and Taylor, 1994). (iii) Daytime R_{eco} is obtained by extrapolating nighttime fluxes using the temperature response. (iv) GPP is calculated as the difference between daytime NEE and R_{eco}; additional checks are performed to avoid unrealistic values of GPP. Finally, a positive NEE indicates an upward flux whereas a negative NEE indicates a downward flux; GPP is positive or zero and R_{eco} is positive. NEE = R_{eco} − GPP.

2.3 Groundwater and surface water monitoring

To compare groundwater carbon dynamics on both the plot and the watershed scales, we selected three piezometers in different forest types (Fig. 1). According to the depth and amplitude of the water table, the three piezometers were representative of dry Landes (piezometer 2), mesophyllous Landes (piezometer 3) and a situation between mesophyllous and wet Landes (piezometer Bilos). Moreover, the piezometer 2 is located in a riparian mixed pine and oak forest near a first-order stream whereas piezometer 3 is located in another pine forest (approximately the same age as the Bilos pine forest). We also selected six first-order streams whose watersheds were dominated largely by pine forest ($\sim 90\,\%$), which limits biogeochemical signal from crops. Shallow groundwater and stream waters were sampled for partial pressure of CO_2 (pCO_2), total alkalinity and DOC with approximately monthly time intervals (Table S1 in the Supplement).

2.4 Chemical analysis

We measured the pCO_2 directly in the field and total alkalinity and DOC back in the laboratory. The pCO_2 in the groundwater and streams was measured directly using an equilibrator (Frankignoulle and Borges, 2001; Polsenaere et al., 2013). This equilibrator was connected to an infrared gas analyzer (LI-COR®, LI-820), which was calibrated one day before sampling, on two linear segments because of its nonlinear response in the range of observed pCO_2 values (0–90 000 ppmv). This nonlinearity was due to saturation of the infrared cell at pCO_2 values above 20 000 ppmv. We used certified standards (Air Liquide™ France) of 2079 ± 42; $19\,500 \pm 390$ and $90\,200 \pm 1800$ ppmv, as well as nitrogen flowing through soda lime for zero. For the first linear segment (0–20 000 ppmv), which corresponded to the river waters, we set the LI-COR (LI-820) to zero and spanned the LI-COR (LI-820) at 19 500 ppmv, and then we checked for linearity at 2042 ppmv. For the second segment (20 000–90 000 ppmv), which corresponded to the sampled groundwater, we measured the response of the LI-COR (LI-820) with the standard at 90 000 ppmv and used this measured value to make a post correction of the measured value in the field. Before sampling, the groundwater was pumped from the piezometer during the time necessary to obtain stable readings with portable probes of electrical conductivity, temperature, pH and dissolved oxygen concentration.

Total alkalinity was analyzed using automated electrotitration on 50 mL filtered samples with 0.1N HCl as the titrant. The equivalence point was determined to be from a pH between 4 and 3 with the Gran method (Gran, 1952). The precision based on replicate analyses was better than $\pm 5\,\mu M$. For samples with a very low pH (< 4.5), we bubbled the water with atmospheric air in order to degas the CO_2. Consequently, the initial pH increased above the value of 5, and total alkalinity titration could be performed (Abril

et al., 2015). We calculated DIC from pCO_2, total alkalinity and temperature measurements using carbonic acid dissociation constants of Millero (1979) and the CO_2 solubility from Weiss (1974) as implemented in the CO_2SYS program (Lewis et al., 1998). Contrary to the pCO_2 calculation from pH and total alkalinity (Abril et al., 2015), the DIC calculation from measured pCO_2 and total alkalinity was weakly affected by the presence of organic alkalinity because 80 ± 20 % of DIC in our samples was dissolved CO_2. The DOC samples were obtained in the field through pre-combusted GF/F filters after filtration (porosity of 0.7 µm). The samples were acidified with 50 µL of HCl 37 % to reach a pH of 2 and stored in pre-combusted Pyrex 25 mL vials at 4 °C in the dark before analysis. The DOC concentrations were measured with a Shimadzu TOC 500 analyzer with repeatability better than 0.1 mg L^{-1}.

2.5 Hydrological monitoring

The precipitation was measured continuously at the Bilos plot using automatic rain gauges with a 30 min integration: one tipping bucket rain gauge SBS500 (Campbell Scientific, Logan, USA) was located in a small clear-cut area at 3 m above ground from 1 January to 10 May 2014 and one total rain weighing sensor, TRwS 405 (MPS system, Bratislava, Slovakia) was located at the top of the canopy on a 6 m tower from 1 July 2014 to 31 December 2015. Hence, between 11 May and 31 June 2014, no precipitation measurements were available at the Bilos site. Thus, during this period, we used data from Météo France© at Belin-Béliet (approximately 30 km from the Bilos site). The precipitation measurements were also checked weekly in the field with manual reports.

The groundwater table depth was measured continuously at the Bilos plot using high-performance level pressure sensors (PDCR/PTX 1830, Druck and CS451451, Campbell Scientific) in one piezometer located at the Bilos site. Temperature and air pressure fluctuations were fully compensated for in the pressure measurements. The measurements were obtained at 60 s intervals and integrated in a 30 min period. They were checked weekly with a manual probe. The groundwater table depth was also measured punctually with a manual piezometric probe in piezometers 2 and 3 before each groundwater sampling.

Our study benefited from four calibrated gauging stations of DIREN (French water survey agency), with a daily temporal resolution, located at two second-order streams (Bourron and Grand Arriou rivers), one third-order stream (Petite Leyre river) and one fourth-order stream (Grande Leyre river) (Fig. 1). We also performed additional discharge measurements in first-order streams (Fig. 1). For each stream order, we calculated the drainage with a daily temporal resolution for a 2-year period (i.e., discharge divided by the corresponding catchment area, in $m^3\,km^{-2}\,day^{-1}$ or in $mm\,day^{-1}$) (Deirmendjian and Abril, 2018). We then determined the increase in drainage between two streams of successive orders. Because of the specific characteristics of the Leyre watershed with no surface runoff, we observed a regular increase in drainage values between two streams of successive orders. In addition, the proportion of additional drainage occurring in each stream order was relatively constant temporally. Our analysis based on daily discharge monitoring in second-, third-, and fourth-order streams and seasonal gauging of first-order streams revealed that monthly drainage values in first-order streams were on average 2.3 times lower than those measured in fourth-order streams and allowed us to reconstruct robust monthly drainage values in first-order streams (Deirmendjian and Abril, 2018). We wrote the water mass balance equation at the Bilos forest plot as follows:

$$P = D + \mathrm{ETR} + \mathrm{GWS} + \Delta S, \quad (1)$$

where P, D, ETR, GWS and ΔS were, respectively, precipitation, drainage, evapotranspiration, groundwater storage and change of soil water content in the unsaturated zone, all expressed in millimeters per day. P was the cumulative precipitation measured over a given period t at the Bilos site. D was the drainage at the Bilos site deduced from daily observation at four gauging stations and the hydrological model (Deirmendjian and Abril, 2018). ETR was the cumulative evapotranspiration obtained from eddy covariance measurements of latent heat fluxes over a period t at the Bilos site. GWS was calculated as the net change in water table depth over the period t times the soil effective porosity at the Bilos site of 0.2 (Augusto et al., 2010; Moreaux et al., 2011). Finally, no reliable measurements of soil water content were available, and with the ΔS term likely being small, the variation in soil water content in the unsaturated zone was neglected in the water mass balance.

2.6 Carbon stocks in groundwater, exports to streams and degassing to the atmosphere

We calculated four different terms that describe the dynamics of carbon at the Bilos plot: the stocks of DIC (DIC_{stock}) and DOC (DOC_{stock}) in groundwater and the exports of DIC (DIC_{export}) and DOC (DOC_{export}) from groundwater to first-order streams, all integrated between two sampling dates (Table S2). Because we do not know the total height of the permeable surface soil layer in piezometers 2 and 3, we calculated the stocks of carbon in the groundwater only at the Bilos site. However, in order to account for spatial differences among the dry, mesophyllous and wet Landes, specific DIC and DOC exports were calculated for the three study site piezometers. We wrote

$$\mathrm{DIC_{stock}} = (S_\mathrm{i} + S_\mathrm{f})\,/\,2 = (\mathrm{DIC_i} \times V_\mathrm{i} + \mathrm{DIC_f} \times V_\mathrm{f})\,/\,2, \quad (2)$$

where DIC_{stock} was the mean stock of DIC in groundwater between two sampling dates in millimoles per square meter. S_f and S_i were the final and the initial stocks of DIC in

Table 1. Water budget on the Bilos plot scale for the years 2014 and 2015, as well as for high flow (January–March 2014 and February–March 2015), growing season (April–August 2014 and April–August 2015), late summer (September–October 2014 and September–October 2015) and early winter (November 2014–January 2015 and November–December 2015). Numbers represent the mean ± SD and the range (in square brackets).

	Precipitation ($mm\,day^{-1}$)	Evapotranspiration ($mm\,day^{-1}$)	Drainage ($mm\,day^{-1}$)	Groundwater storage ($mm\,day^{-1}$)
2014	3.0 ± 2.1	2.5 ± 1.4	0.5 ± 0.5	-0.2 ± 2.3
	[0.2–8.0]	[0.3–5.3]	[0.1–1.9]	[−2.9–4.5]
2015	1.9 ± 1.2	1.7 ± 1.0	0.3 ± 0.3	-0.5 ± 1.9
	[0.2–4.1]	[0.3.–3.4]	[0.1–0.9]	[−3.1–2.6]
High flow	4.7 ± 2.1	2.4 ± 1.0	1.1 ± 0.4	−0.2
	[2.2–8.0]	[0.9–3.6]	[0.7–1.9]	[−2.9–4.0]
Growing season	1.8 ± 0.8	3.0 ± 0.9	0.3 ± 0.2	−1.9
	[0.8–2.9]	[1.6–5.3]	[0.1–0.7]	[−3.1—0.5]
Late summer	1.1 ± 0.5	1.5 ± 0.5	0.1 ± 0.007	0.1
	[0.2–1.5]	[1.0–2.2]	[0.1–0.1]	[−1.2–0.7]
Early winter	2.7 ± 1.5	0.5 ± 0.2	0.2 ± 0.07	1.9
	[0.2–4.7]	[0.3–0.7]	[0.1–0.3]	[0.7–4.5]

groundwater in millimoles per square meter. DIC_i and DIC_f were the initial and the final concentration of DIC in groundwater in millimoles per cubic meter, respectively. V_i and V_f were the initial and the final volumes of groundwater in cubic meters per square meter. The volume of groundwater (V) was calculated as follows:

$$V = (h + H) \times \Phi_{\text{effective}}, \quad (3)$$

where h and H (H is negative) were the total height of the permeable surface layer (equals to 10 m; Corbier et al., 2010) and the height of groundwater table, respectively. $\Phi_{\text{effective}}$ was the effective porosity of the soil and it was equal to 0.2. Export of DIC in first-order streams through drainage of shallow groundwater was calculated from discharge and concentration as follows:

$$DIC_{\text{export}} = D \times (DIC_i + DIC_f) / 2, \quad (4)$$

where D was the mean drainage of shallow groundwater by first-order streams between the initial and the final sampling dates in meters per day. DIC_i and DIC_f were the initial and final concentrations of DIC in groundwater in millimoles per cubic meter. We calculated DOC_{stock} and DOC_{export} in the same manner as DIC_{stock} and DIC_{export}. In addition, we also calculated the DIC exported from first-order streams to second-order streams by replacing the concentrations of carbon in the groundwater with the carbon concentrations in first-order streams in Eq. (4). Between two sampling dates, the degassing of CO_2 in first-order streams could thus be obtained from the difference between the DIC exported from groundwater and from first-order streams.

3 Results

3.1 Hydrological parameters and water mass balance

Water mass balance at the Bilos site was calculated on a monthly basis over a 2-year period (2014–2015) (Table 1; Figs. 2c–3). Monthly precipitation on the one hand and the sum of evapotranspiration, groundwater storage and drainage on the other hand closely followed the 1 : 1 line (Fig. 3), showing the consistency of the water mass balance estimated with different techniques and independent devices, even with a monthly temporal resolution insufficient to account for very sudden processes. During the years 2014 and 2015, we could define four different hydrological periods that were high-flow, growing season, late summer and early winter periods (Fig. 2). High-flow periods were characterized by two relatively short flood events in January–March 2014 (peak of $120\,m^3\,s^{-1}$) and in February–March 2015 (peak of $80\,m^3\,s^{-1}$), high drainage values (maximum of $1.9\,mm\,day^{-1}$ in February 2014) and a water table close to the soil surface (Table 1; Fig. 2a, c). These short periods of high flow in winter were followed by the forest growing season in spring and summer in May 2014–August 2014 and April–August 2015 characterized by the highest GPP and R_{eco} (peak of 880 and $660\,mmol\,m^{-2}\,day^{-1}$, respectively, in May 2015) and highest evapotranspiration (peak of $5.3\,mm\,day^{-1}$ in April 2014); during this forest growing period, the groundwater table decreased and groundwater storage was negative (Tables 1, 3; Fig. 2). Growing season periods were followed by late summer periods that were characterized by low precipitations (minimum of $0.2\,mm\,day^{-1}$ in September 2014) and the lowest groundwater table depth in September–October 2014 and in September–October 2015 (Table 1; Fig. 2a, c). Then, late summer periods were fol-

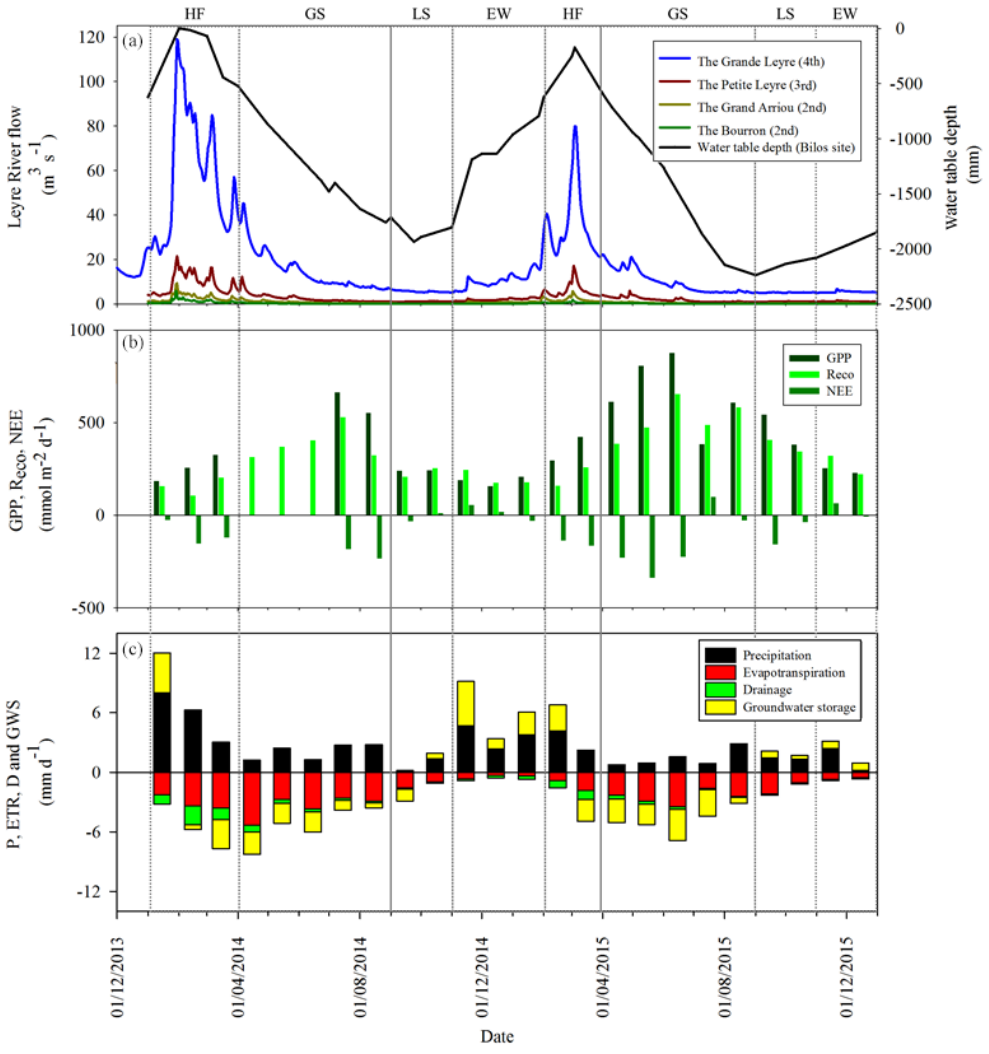

Figure 2. Seasonal variations in hydrological parameters in the Leyre watershed. **(a)** Discharge of the Grande Leyre, the Petite Leyre, the Grand Arriou and the Bourron rivers associated with water table at the Bilos site. **(b)** Metabolic parameters (NEE, GPP, R_{eco}) estimated at the Bilos site. **(c)** Monthly precipitation, evapotranspiration and groundwater storage at the Bilos site as well as the drainage of first-order streams. Inputs of water (precipitation and positive groundwater storage) in the studied ecosystem are represented on a positive scale whereas outputs of water (drainage, evapotranspiration and negative groundwater storage) are represented on a negative scale. HF, GS, LS and EW represent high-flow (January–March 2014 and February–March 2015), growing season (April–August 2014 and April–August 2015), late summer (September–October 2014 and September–October 2015) and early winter (November 2014–January 2015 and November–December 2015) periods, respectively.

lowed by early winter periods that were associated with heavy precipitations (peak of 4.7 mm day^{-1} in November 2014) and a rising groundwater table (positive groundwater storage) in November 2014–January 2015 and in November–December 2015 (Table 1; Fig. 2a, c). We considered that growing season and late summer and early winter periods, merged together represented periods of base flow.

Periods of groundwater discharge with negative groundwater storage (February–September 2014 and March–August 2015) were characterized by evapotranspiration higher than precipitation (Fig. 2a, c). Conversely, periods of groundwater recharge with positive groundwater storage (October 2014–February 2015 and September–December 2015) were characterized by precipitations higher than evapotranspiration (Fig. 2a, c). Consequently, on the plot scale, significant correlation between groundwater storage and precipitations and between groundwater storage and evapotranspiration were observed (Table 2), attesting to evapotranspiration and precipitation playing a significant role in the groundwater storage.

Table 2. Linear correlation (Pearson) between the studied parameters on the Bilos plot scale during the sampling period. Numbers represent the Pearson's correlation coefficient at the Bilos plot between mean carbon concentrations (mmol m^{-3}) in the Bilos groundwater and in the six first-order streams, carbon stocks (mmol m^{-2} day^{-1}), carbon exports (mmol m^{-2} day^{-1}), carbon degassing (mmol m^{-2} day^{-1}) in the six first-order streams, hydrological parameters (mm day^{-1}, which are P, GWS, ETR and D for precipitation, groundwater storage, evapotranspiration and drainage, respectively), water table depth (mm) and metabolic parameters (mmol m^{-2} day^{-1}). Here, degassing was calculated from the DIC data of the Bilos groundwater only. Each parameter was integrated between two sampling dates (Table S2). Values in bold font indicate correlation with a p value < 0.05, whereas values in italic font indicate correlation with a p value < 0.001.

	Concentration in groundwater (mmol m^{-3})		Concentration in streams (mmol m^{-3})		Stock in groundwater (mmol m^{-2})		Export from groundwater to streams (mmol m^{-2} day^{-1})		Degassing in streams (mmol m^{-2} day^{-1})	Hydrological parameters (mm day^{-1})				Water table depth (mm)	Metabolic parameters (mmol m^{-2} day^{-1})		
	DIC_{gw}	DOC_{gw}	DIC_{stream}	DOC_{stream}	DIC_{stock}	DOC_{stock}	DIC_{export}	DOC_{export}	F_{degass}	P	GWS	ETR	D	H	NEE	GPP	R
DIC_{gw}	1	**−0.65**	*0.86*	−0.34	*0.99*	**−0.65**	−0.44	**−0.62**	−0.48	−0.02	0.45	−0.41	**−0.68**	*−0.83*	**0.52**	−0.31	−0.09
DOC_{gw}		1	−0.41	0.43	**−0.64**	*0.98*	**0.69**	*0.95*	**0.56**	0.17	−0.28	0.41	*0.93*	*0.85*	−0.19	−0.13	−0.36
DIC_{stream}			1	**−0.55**	*0.82*	−0.42	−0.35	−0.34	**−0.54**	−0.14	0.23	−0.25	−0.44	**−0.75**	0.43	−0.32	−0.16
DOC_{stream}				1	−0.33	0.45	0.45	0.38	**0.66**	0.30	0.35	−0.39	0.46	**−0.70**	0.15	−0.41	**−0.53**
DIC_{stock}					1	**−0.63**	0.37	**−0.62**	−0.44	−0.04	0.45	−0.44	**0.67**	**−0.79**	−0.48	0.28	−0.07
DOC_{stock}						1	*−0.82*	*0.97*	**0.67**	0.21	−0.23	0.32	*−0.97*	*0.88*	0.20	−0.14	−0.39
DIC_{export}							1	**0.72**	*0.86*	0.26	0.01	0.02	*0.83*	**0.76**	−0.18	−0.15	−0.39
DOC_{export}								1	**0.57**	0.24	−0.22	0.28	*0.98*	*0.81*	−0.19	−0.17	−0.41
F_{degass}									1	0.45	0.24	0.17	**0.70**	*0.78*	0.06	−0.35	**−0.50**
P										1	**0.76**	−0.30	0.29	0.23	0.33	−0.44	−0.43
GWS											1	**−0.73**	−0.16	−0.15	**0.62**	**−0.63**	**−0.51**
ETR												1	0.22	0.17	**−0.63**	**0.63**	**0.50**
D													1	*0.88*	−0.23	−0.15	−0.41
H														1	−0.27	−0.06	0.31
NEE															1	*−0.85*	**−0.55**
GPP																1	*0.91*
R																	1

Table 3. Metabolic parameters (GPP, R_{eco} and NEE) estimated at the Bilos plot with the eddy covariance techniques. Numbers represent the mean ± SD and the range (between square brackets) for the years 2014–2015 and for high-flow (January–March 2014 and February–March 2015), growing season (April–August 2014 and April–August 2015), late summer (September–October 2014 and September–October 2015) and early winter (November 2014–January 2015 and November–December 2015) periods. Positive NEE indicates an upward flux whereas a negative NEE indicates a downward flux; GPP is positive or zero and R_{eco} is positive. NEE = $R_{eco.}$ − GPP.

	GPP ($mmol\,m^{-2}\,day^{-1}$)	R_{eco} ($mmol\,m^{-2}\,day^{-1}$)	NEE ($mmol\,m^{-2}\,day^{-1}$)
2014–2015	400 ± 210	310 ± 150	−90 ± 110
	[160–880]	[110–660]	[−340–100]
High flow	300 ± 80	180 ± 50	−120 ± 50
	[180–420]	[105–260]	[−160—30]
Growing season	640 ± 150	490 ± 100	−160 ± 140
	[380–880]	[320–640]	[−330–100]
Late summer	350 ± 120	300 ± 80	−50 ± 60
	[240–540]	[200–410]	[−160–10]
Early winter	210 ± 30	230 ± 50	20 ± 20
	[160–260]	[170–320]	[−10–65]

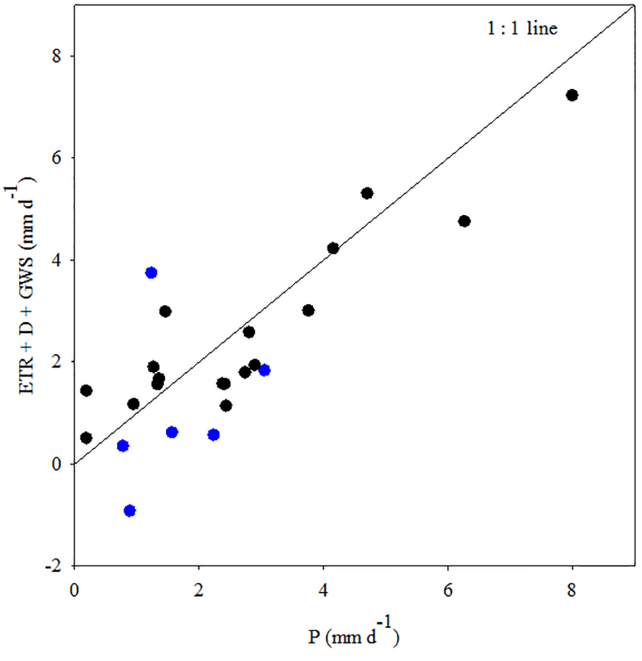

Figure 3. Monthly water mass balance at the Bilos site for the 2014–2015 period. Pearson coefficient $R = 0.85$ and p value < 0.001. Blue points represent months when groundwater storage was extremely negative in March 2014, April 2014, March 2015, April 2015, June 2015 and July 2015 (Fig. 2c). These blue points are further away from the 1 : 1 line than the other months (represented in black). The drainage of the Leyre river is delayed compared to the drainage of the Bilos plot. Thus, when the loss of groundwater is extremely high (negative groundwater storage), estimated drainage does not correspond exactly to the measured groundwater storage.

3.2 Net ecosystem exchange of CO_2 in the forest plot (Bilos plot)

GPP, R_{eco} and NEE exhibited a strong seasonal variability (Table 3; Fig. 2b). GPP, R_{eco} and NEE were 400 ± 220, 310 ± 150 and −90 ± 110 $mmol\,m^{-2}\,day^{-1}$, respectively, throughout the years 2014 and 2015 (we excluded the 16 May–7 July 2014 period when no eddy covariance measurements were available), equivalent to 1750 ± 960, 1360 ± 660 and 390 ± 480 $g\,C\,m^{-2}\,yr^{-1}$ (Table 3; Fig. 2b). These results were close to Moreaux et al. (2011) estimates of 1720, 1480 and 340 $g\,C\,m^{-2}\,yr^{-1}$ as measured at a younger forest stage in the same forest plot. GPP increased from early winter (210 ± 30 $mmol\,m^{-2}\,day^{-1}$) to growing season (640 ± 150 $mmol\,m^{-2}\,day^{-1}$) periods (Table 3; Fig. 2b). R_{eco} followed the same temporal trend (Table 3; Fig. 2b). During late summer and early winter periods, NEE could be positive (R_{eco} > GPP), meaning that the pine forest ecosystems had switched from autotrophic to heterotrophic metabolism, notably in October, November and December 2014 (Table 3; Fig. 2b). NEE was always negative (R_{eco} < GPP) during high-flow and growing season periods, except in July 2015, probably as a consequence of temporary low precipitation (Table 3; Fig. 2b–c).

3.3 Dissolved carbon evolution in shallow groundwater

In shallow groundwater, total alkalinity was low and originated from slow weathering of silicate minerals with vegetation-derived CO_2 (Polsenaere and Abril, 2012). The mean proportion of total alkalinity in the DIC pool in shallow groundwater was 5 %, the large majority of the DIC being composed of dissolved CO_2 resulting from microbial and plant root respiration in the soil. Although the sampling frequency was monthly or more, it allowed the detection of significant changes in the groundwater DIC and DOC con-

Table 4. Carbon concentrations in the sampled groundwater and in the sampled first-order streams during the sampling period (January 2014–July 2015) for high-flow (January–March 2014 and February–March 2015), growing season (April–August 2014 and April–August 2015), late summer (September–October 2014 and September–October 2015) and early winter (November 2014–January 2015 and November–December 2015) periods. Numbers represent the mean ± SD, the range (between square brackets) and the number (N) of samples for each hydrological period.

	DOC (mmol m^{-3})				DIC (mmol m^{-3})			
	Piezometer Bilos	Piezometer 2	Piezometer 3	Streams	Piezometer Bilos	Piezometer 2	Piezometer 3	Streams
High flow	3500 ± 200 [3200–3700] $N = 3$	280 $N = 1$	1500 $N = 1$	490 ± 10 [460–510] $N = 15$	1160 ± 470 [570–1700] $N = 3$	1380 $N = 1$	1510 $N = 1$	280 ± 40 [220–310] $N = 15$
Growing season	750 ± 440 [320–950] $N = 7$	380 ± 40 [300–400] $N = 5$	880 ± 400 [550–830] $N = 4$	360 ± 100 [200–540] $N = 41$	2570 ± 240 [2350–3030] $N = 7$	1450 ± 380 [1000–2100] $N = 5$	2030 ± 220 [1650–2160] $N = 4$	330 ± 120 [210–550] $N = 41$
Late summer	540 ± 60 [480–600] $N = 2$	420 ± 80 [340–500] $N = 2$	$N = 0$	370 ± 30 [340–400] $N = 4$	5240 ± 140 [5100–5400] $N = 2$	3900 ± 100 [3800–4000] $N = 2$	$N = 0$	1030 ± 240 [790–1270] $N = 4$
Early winter	640 ± 50 [580–670] $N = 3$	470 ± 110 [350–620] $N = 3$	760 $N = 1$	510 ± 30 [480–550] $N = 17$	2600 ± 980 [1850–4000] $N = 3$	2370 ± 1500 [940–4500] $N = 3$	2040 $N = 1$	300 ± 90 [240–430] $N = 17$

centrations, consistent from one year to another at Bilos site and from one site to another during the second hydrological year of the study (Figs. 4–5). One first and relevant key result was the opposite temporal evolution of DIC and DOC concentrations in groundwater with water table depth (Table 2; Figs. 4–5). Indeed, DIC and DOC concentrations in groundwater exhibited strong temporal variations in relation with the hydrological cycle (Table 4; Figs. 4–5). On the one hand, during high-flow and growing season periods of 2014, the increase in DIC in Bilos groundwater (570 to 3030 µmol L^{-1}) was associated with a fast decrease in DOC in Bilos groundwater (3625 to 950 µmol L^{-1}), in parallel with a decline in the water table (Fig. 5). In 2015, the same temporal trend was observed at the same period, but with a lesser extent (Fig. 5). On the other hand, during late summer, the increase in DIC concentrations in Bilos groundwater (2700 to 5400 µmol L^{-1}) was this time not related with any decrease in DOC concentrations in groundwater (Fig. 5b–c). This maximum of DIC concentrations in groundwater corresponded to the late summer period when the overlaying forest ecosystem had switched from autotrophic to heterotopic metabolism (Figs. 2b, 5). During early winter and high-flow periods, DIC concentrations in Bilos groundwater decreased from 4000 µmol L^{-1} (November 2014) to 1700 µmol L^{-1} (March 2015), in parallel with a rise in the water table (Fig. 5a–b). Concomitantly, a fast increase in DOC concentrations from 670 to 3600 µmol L^{-1} occurred in Bilos groundwater between the same time periods (Fig. 5a, c).

The DIC concentrations in the three sampled piezometers exhibited a modest spatial heterogeneity (Table 4; Fig. 5b). DIC concentrations were low (e.g., 570 µmol L^{-1} in the Bilos piezometer in February 2014) during periods of high flow and were high (e.g., 5370 µmol L^{-1} in the Bilos piezometer

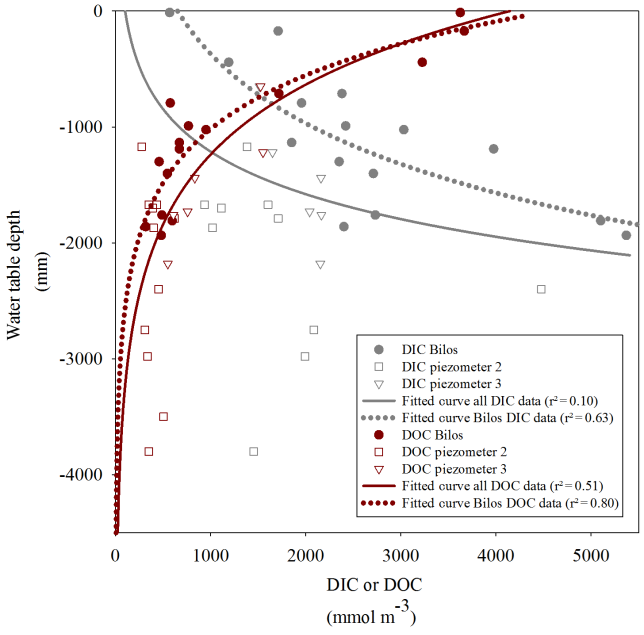

Figure 4. The concentrations of DIC and DOC in the three sampled groundwaters as a function of water table depth.

in September 2014) during late summer (Table 4; Fig. 5a–b). In contrast to DIC, the DOC concentrations exhibited a significant spatial heterogeneity, particularly during high-flow periods (Table 4; Fig. 5b–c). During these periods of high flow, DOC concentrations were higher in the Bilos piezometer (3800 ± 200 µmol L^{-1}) than in piezometers 2 (280 µmol L^{-1}) and 3 (1500 µmol L^{-1}) (Table 4; Fig. 5a, c). During the other hydrological periods (periods of base flow), DOC concentrations in piezometer 2 were still lower than the

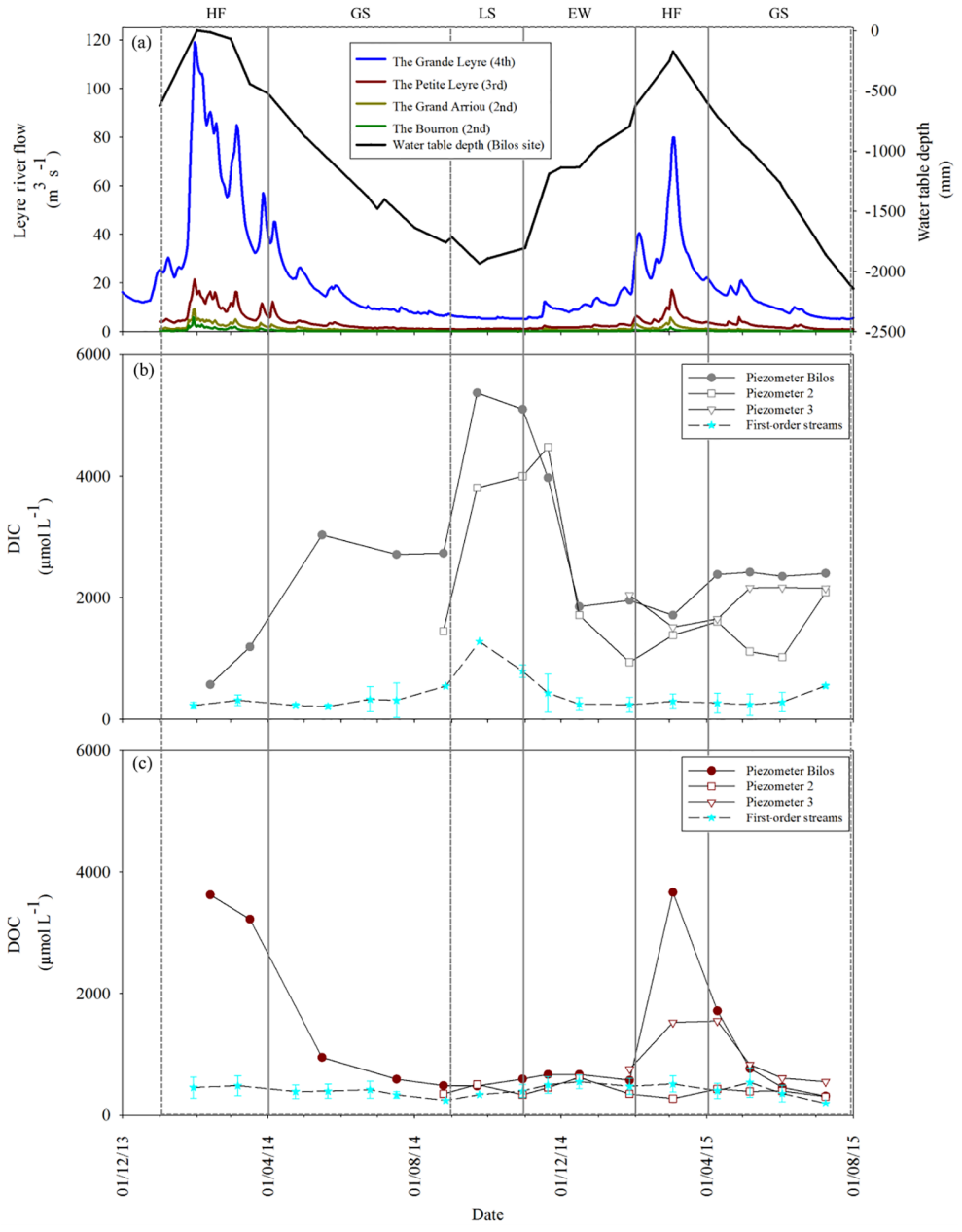

Figure 5. (a) Discharge of the Grande Leyre, the Petite Leyre, the Grand Arriou and the Bourron rivers associated with the water table at the Bilos site. Temporal variations throughout the sampling period in **(b)** the DIC concentrations, in the sampled piezometers, in the sampled first-order streams (medium dashed line; errors bars represent standard deviation of the six first-order streams), and in **(c)** the DOC concentrations, in the sampled piezometers and in the sampled first-order streams (medium dashed line; errors bars represent standard deviation of the six first-order streams). HF, GS, LS and EW represent high-flow (January–March 2014 and February–March 2015), growing season (April–August 2014 and April–August 2015), late summer (September–October 2014 and September–October 2015) and early winter (November 2014–January 2015 and November–December 2015) periods, respectively.

two other piezometers (Bilos and 3) (Table 5). However, during periods of base flow, groundwater DOC concentrations at the three sampled sites remained more or less constant (Table 4; Fig. 5a, c).

3.4 Dissolved carbon evolution in first-order streams

In first-order streams, the DIC concentrations exhibited smaller temporal variations and significantly lower values than in groundwater, attesting to degassing occurring at the groundwater–stream interface (Table 4; Fig. 5b). In contrast

Table 5. Export of DIC and DOC from the sampled groundwater to first-order streams, as well as degassing in first-order streams, for the sampling period and for high-flow (January–March 2014 and February–March 2015), growing season (April–August 2014 and April–August 2015), late summer (September–October 2014 and September–October 2015) and early winter (November 2014–January 2015 and November–December 2015) periods. Numbers represent the mean ± SD whereas numbers in square brackets represent the range. Here, degassing was calculated with the DIC data from the three sampled groundwaters.

	DOC_{export} ($mmol\,m^{-2}\,day^{-1}$)				DIC_{export} ($mmol\,m^{-2}\,day^{-1}$)				Degassing ($mmol\,m^{-2}\,day^{-1}$)
	Bilos piezometer	Piezometer 2	Piezometer 3	Streams[b]	Bilos piezometer	Piezometer 2	Piezometer 3	Streams[b]	Streams
High flow	3.4 ± 1.1 [2.3–4.9]	0.4 ± 0.02 [0.3–0.4]	1.5 ± 0.2 [1.2–1.7]	0.6 ± 0.1 [0.5–0.7]	1.8 ± 0.4 [1.3–2.2]	1.4 ± 0.2 [1.3–1.6]	1.8 ± 0.1 [1.7–1.9]	0.3 ± 0.1 [0.3–0.4]	1.4 ± 0.2 [0.8–1.9]
Growing season	0.4 ± 0.4 [0.1–1.2]	0.05 ± 0.02 [0.1–0.2]	0.2 ± 0.2 [0.1–0.4]	0.1 ± 0.1 [0.05–0.3]	0.7 ± 0.3 [0.4–1.3]	0.3 ± 0.1 [0.3–0.5]	0.6 ± 0.1 [0.4–0.7]	0.1 ± 0.03 [0.05–0.2]	0.5 ± 0.2 [0.3–1.3]
Late summer	0.1 ± 0.01 [0.1–0.1]	0.1 ± 0.04 [0.1–0.1]		0.1 ± 0.01 [0.05–0.1]	0.6 ± 0.03 [0.6–0.7]	0.4 ± 0.05 [0.4–0.5]		0.1 ± 0.01 [0.1–0.1]	0.4 ± 0.1 [0.4–0.6]
Early winter	0.1 ± 0.02 [0.1–0.2]	0.1 ± 0.03 [0.1–0.1]	0.2	0.1 ± 0.02 [0.1–0.1]	0.7 ± 0.1 [0.5–0.8]	0.6 ± 0.2 [0.4–0.8]	0.6	0.1 ± 0.02 [0.1–0.1]	0.5 ± 0.1 [0.5–0.6]
2014–2015	0.9 ± 1.4 [0.1–4.9]	0.1 ± 0.1 [0.05–0.4]	0.6 ± 0.5 [0.1–1.7]	0.2 ± 0.2 [0.05–0.7]	0.9 ± 0.5 [0.4–2.2]	0.6 ± 0.4 [0.3–1.6]	1.0 ± 0.6 [0.4–1.9]	0.2 ± 0.1 [0.05–0.4]	0.6 ± 0.3 [0.2–1.3]
Entire watershed (2014–2015)		0.7 ± 0.7[a]		0.2 ± 0.2		0.9 ± 0.5[a]		0.2 ± 0.1	0.7 ± 0.5

[a] Mean carbon export weighted by surface, assuming that the Bilos piezometer is representative of the wet Landes, that piezometer 2 is representative of the dry Landes and that piezometer 3 is representative of the mesophyllous Landes using the relative surface area of each type of Landes. [b] Carbon exports from first- to second-order streams calculated from the drainage of first-order streams ($mm\,day^{-1}$) and the mean concentrations of DOC and DIC in first-order streams ($mmol\,m^{-3}$).

to DIC, the DOC concentrations in first-order streams were of the same order of magnitude as in piezometer 2 (dry Landes) and significantly lower than in the two other piezometers (wet to mesophyllous Landes), in particular during periods of high flow (Table 4; Fig. 5c). As in groundwater, DOC and DIC concentrations in first-order streams were significantly anticorrelated (Table 2), suggesting that carbon dynamics in first-order streams was mostly impacted by groundwater inputs.

3.5 Carbon stocks in groundwater and exports to streams

At the Bilos site, the stocks of DIC and DOC in groundwater followed the same temporal trend as DIC and DOC concentrations (Figs. 5–6). The stock of DIC increased from high-flow ($1140\,mmol\,m^{-2}$ the 12 February 2014) to late summer ($8700\,mmol\,m^{-2}$ the 24 September 2014) periods, whereas at the same time intervals, the stock of DOC decreased from 7240 to $780\,mmol\,m^{-2}$ (Fig. 6). Furthermore, between 12 February and 16 May 2014 (95 days), we observed an increase of $4500\,mmol\,m^{-2}$ in DIC stocks very close to the decrease in DOC stocks of $5500\,mmol\,m^{-2}$. This suggests that during the following months after the DOC peak in groundwater at high-flow period, DOC is degraded to DIC within the groundwater itself. During this period, the degradation rate of DOC in the groundwater could be estimated at approximately $60\,mmol\,m^{-2}\,day^{-1}$.

The export of DOC occurred mostly during high-flow periods (e.g., 90 % of the total DOC export in the Bilos plot occurred during high-flow periods), for each sampled groundwater (Table 5). During high-flow periods, the groundwater DOC concentrations and exports exhibited an important spatial heterogeneity at the three sampled sites (Table 5). During these periods of high flow, DOC export was higher in the Bilos piezometer ($3.4 \pm 1.1\,mmol\,m^{-2}\,day^{-1}$) than in piezometer 2 ($0.4 \pm 0.02\,mmol\,m^{-2}\,day^{-1}$) and in piezometer 3 ($1.5 \pm 0.2\,mmol\,m^{-2}\,day^{-1}$) (Table 5). These contrasts in DOC exports were related to the water table depth and amplitude (Fig. 4) and the gradient in soil carbon between the different podzols. In contrast to DOC exports, approximately the same quantity of DIC was exported during high-flow periods (e.g., 50 % of the total DIC export in the Bilos plot occurred during high-flow periods) as during the other hydrological periods for each sampled groundwater (Table 5). Groundwater DIC exports exhibited a smaller spatial heterogeneity than DOC exports although DOC and DIC concentrations showed opposite seasonal trends in groundwater (Tables 4–5, Fig. 5b–c); the time-integrated value of carbon export for the sampling period was $0.9 \pm 0.5\,mmol\,m^{-2}\,day^{-1}$ ($3.9 \pm 2.2\,g\,C\,m^{-2}\,yr^{-1}$) for DIC and $0.7 \pm 0.7\,mmol\,m^{-2}\,day^{-1}$ ($3.1 \pm 3.1\,g\,C\,m^{-2}\,yr^{-1}$) for DOC (Table 5). As drainage of groundwater was the only hydrological pathway in the Leyre watershed, terrestrial carbon leaching to streams was estimated to be $1.6 \pm 0.9\,mmol\,m^{-2}\,day^{-1}$ ($7.0 \pm 3.9\,g\,C\,m^{-2}\,yr^{-1}$).

3.6 Degassing in first-order streams

Degassing in first-order streams was $0.7 \pm 0.5\,mmol\,m^{-2}\,day^{-1}$ ($3.1 \pm 2.2\,g\,C\,m^{-2}\,yr^{-1}$) throughout the sampling period (Table 5). Degassing

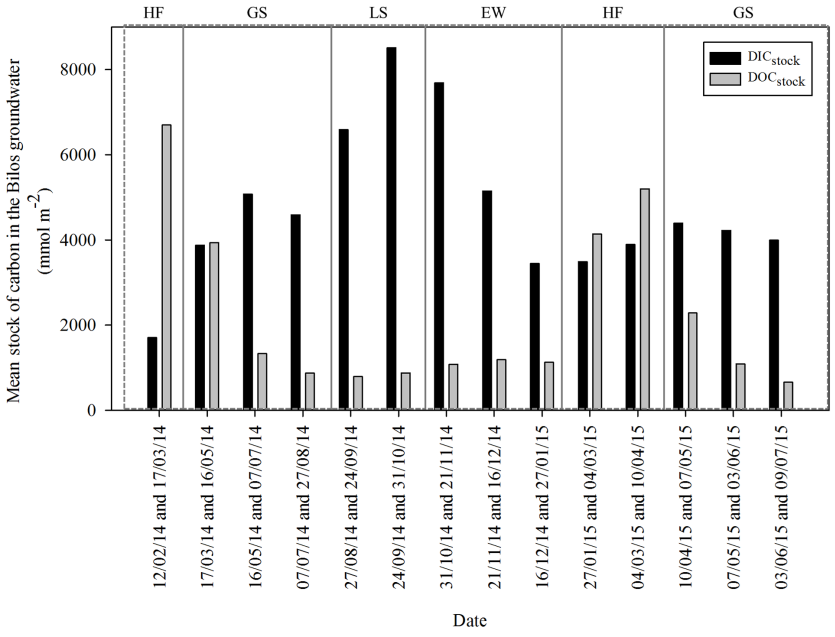

Figure 6. The mean DIC and DOC stocks between two sampling dates in Bilos groundwater. HF, GS, LS and EW represent high-flow (January–March 2014 and February–March 2015), growing season (April–August 2014 and April–August 2015), late summer (September–October 2014 and September–October 2015) and early winter (November 2014–January 2015 and November–December 2015) periods, respectively.

was more important during periods of high flow than during the other hydrological periods (Table 5). In addition, degassing in first-order streams was positively correlated to the export of DIC (Table 2), revealing that degassing was mostly impacted by groundwater inputs. Over a hydrological year, 75 % of the DIC exported from the Leyre watershed based on the three groundwater sampling sites almost immediately returned in the atmosphere through CO_2 degassing in first-order streams (Table 5).

4 Discussion

4.1 Water mass balance and the role of groundwater in the hydrological carbon export

Our hydrological dataset monitored continuously during 18 months allows us to separate the water budget in four terms on the monthly timescale (Table 1; Figs. 2c–3). The water budget at the Bilos plot was primarily impacted by precipitation and evapotranspiration (Table 1; Fig. 2c).

The transfer of precipitation to rivers involves temporary water storage in groundwater (Alley et al., 2002; Oki and Kanae, 2006). However, the lag time between precipitation and groundwater storage was short at our study site, as attested to by the significant correlation between these two parameters (Table 2). Thus, when precipitation is high (during early winter and high-flow periods), water infiltration in the sandy podzols is faster than water capture by vegetation. Consequently, rainwater infiltration rapidly causes the water table to rise and thus increases the groundwater storage (Fig. 2a, c). This fast infiltration is due to the sandy permeable texture of soils with a low soil water retention (Augusto et al., 2010; Vernier and Castro, 2010).

The evapotranspiration was high during the growing season and late summer periods when the precipitation was low (Table 1; Fig. 2c). For that reason, the groundwater storage decreases with increasing evapotranspiration (Table 2; Fig. 2c), revealing that soil water uptake by the pine trees directly lowers the water table. Soil water retention properties usually vary with depth and thus soil water uptake by plant roots generally occurs from areas in the soil with the highest water potential (Domec et al., 2010; Warren et al., 2005). Previous studies suggest that the ordinary soil depth at which most water is taken up in pines is usually 30–40 cm (Klein et al., 2014; Querejeta et al., 2001) where nutrient concentrations are also the highest (Achat et al., 2008). In an experimental Scots pine plot in a flat and sandy area of Belgium, similar to our study site, Vincke and Thiry (2008) reported that water table uptake could contribute to 60 % of the evapotranspiration thanks to capillary rise from the groundwater to the rooted soil layers. Contrary to the pine trees, direct groundwater table uptake has been observed for deciduous trees in a flat and sandy area of Portugal (Mendes et al., 2016), a process that occurred through a dimorphic root system, which allows the access and use of groundwater resources (David et al., 2013) in particular during drought pe-

riods (Del Castillo et al., 2016). Evapotranspiration strongly controls the groundwater storage in pine forests and, as a result, the water table generally rises after clear-cutting (Bosch and Hewlett, 1982; Sun et al., 2000; Xu et al., 2002). At our study site, drainage also significantly increased after wood harvesting due to reduced evapotranspiration, (Kowalski et al., 2003; Loustau and Guillot, 2009). Indeed, the network of drainage ditches created by foresters very rapidly redirects the excess water when the groundwater level rises (Thivolle-Cazat and Najar, 2001). Since most pine roots are located in the first meter of the soil to avoid winter anoxia caused by a rising water table (Bakker et al., 2006, 2009), the pine trees did not exhibit any transpiration reduction when the groundwater level was high (Fig. 2a, c; Loustau et al., 1990).

We observed a lag time between groundwater storage and drainage at our study site (Figs. 2a, c–3), confirmed by the non-significant correlation between these two parameters (Table 2). This lag of 2–3 months was due to the time necessary for water to travel through the soil depending on the spatial temporal gradient of hydraulic head, hydraulic conductivity and porosity of the system (Ahuja et al., 2010; Alley et al., 2002). At our study site, shallow groundwater acts as a buffer system, the drainage mostly being controlled by water table depth and the capacity of the porous soil to store or export water (Alley et al., 2002). Indeed, groundwater flow in a shallow sandy aquifer is largely controlled by the drainage pattern of the streams and ditches and thus by the water table depth and topography of the area (Vissers and van der Perk, 2008). At our study site, the buffer capacity of groundwater explains why the Leyre river discharge increased only in late winter, 2–3 months after the start of high precipitation and water table rise (Fig. 2a, c). Sudden hydrological events are thus buffered by this temporary groundwater storage in the porous soil. As a consequence, temporary groundwater storage mediates almost all the carbon exports to the watershed. Moreover, storms would not have such a crucial impact on the way we estimate carbon exports from groundwater to first-order streams based on monthly sampling frequency. Indeed, with our monthly resolution we observed consistent seasonal effect of DIC and DOC in shallow groundwater and streams (Fig. 5), representative for the different processes that control carbon dynamics in groundwater. Conversely, in steeper and less permeable catchments, carbon exports are quickly affected by storms and pulsed hydrological events (e.g., Raymond and Saiers, 2010; Wilson et al., 2013). Finally, the water mass balance on the Bilos plot scale being consistent with drainage modeled on the watershed scale (Figs. 2c–3), we used this drainage to estimate carbon exports on the plot scale (Table 5).

4.2 Soil carbon leaching to groundwater

Dissolved carbon concentrations varied considerably in groundwater (Table 4; Figs. 4–5) according to seasonal changes in hydrology and forest metabolism and depending on the characteristics of the sampling site. Because the sampling frequency was approximately 1 month, we may have lost some short transitional periods significant for the annual carbon budget. This is most probable during the short period of high flow, when DOC mobilization and export were the highest (Table 5). However, the sampling frequency was sufficient to detect the major trends in groundwater DIC and DOC concentrations, consistent from one hydrological cycle to another at the Bilos site and from one site to another during the second hydrological year of the study, although topographic differences explained spatial differences in DOC and DIC concentrations (Fig. 5). Thanks to the high permeability of the soil and the buffering capacity of the groundwater in response to hydrology, we could observe distinct biogeochemical processes that govern carbon leaching throughout the hydrological cycle.

Dissolved organic matter generally includes a small proportion of low-molecular-weight compounds such as carbohydrates and amino acids and a larger proportion of complex, high-molecular-weight compounds (Evans et al., 2005; Kawasaki et al., 2005). Dissolved organic matter is often quantified by its carbon content and referred to as DOC and nearly all DOC in soils comes from photosynthesis (Bolan et al., 2011). Indeed, DOC in soils in forests originates from throughfall and stemflow, leaf litter leaching, root exudation and decaying fine roots in soils (Bolan et al., 2011). However, a large fraction of DOC in soil solution is sorbed onto minerals and, before being exported to streams, DOC must be mobilized from the soil (Sanderman and Amundson, 2009). Surface precipitation has been described as an important process that transports DOC downward from the topsoil to the saturated zone (Kawasaki et al., 2005; Shen et al., 2015). The transfer of DOC in groundwater also depends on the level of hydraulic connectivity between subsoil horizons and water table depth (Kalbitz et al., 2000). However, up to 90 % of surface-derived DOC can be removed by re-adsorption to minerals prior to reaching the saturated zone (Shen et al., 2015). Furthermore, when sorptive retention of DOC occurs, it contributes to carbon accumulation in subsoils due to the stabilization of organic matter against biological degradation (Kaiser and Guggenberger, 2000; Kalbitz and Kaiser, 2008). During base-flow conditions, the DOC concentrations in groundwater were relatively stable at our study sites, even after rainy periods (Table 4; Figs. 2c, 5c), which suggests that soil DOC in upper horizons was not preferentially mobilized to groundwater by rainwater infiltration. Spatially, groundwater DOC was on average higher at the mesophyllous to wet Landes station (Bilos and piezometer 3), than at the dry Landes (piezometer 2) during periods with a low water table (Table 4). Indeed, several studies have reported decreasing DOC concentrations in groundwater in concurrence with increasing subsoil thickness and water table depth (Datry et al., 2004; Goldscheider et al., 2006; Pabich et al., 2001), with DOC concentrations at or close to zero reported in deep (> 1 km) and old groundwater (Pabich et al., 2001). At our

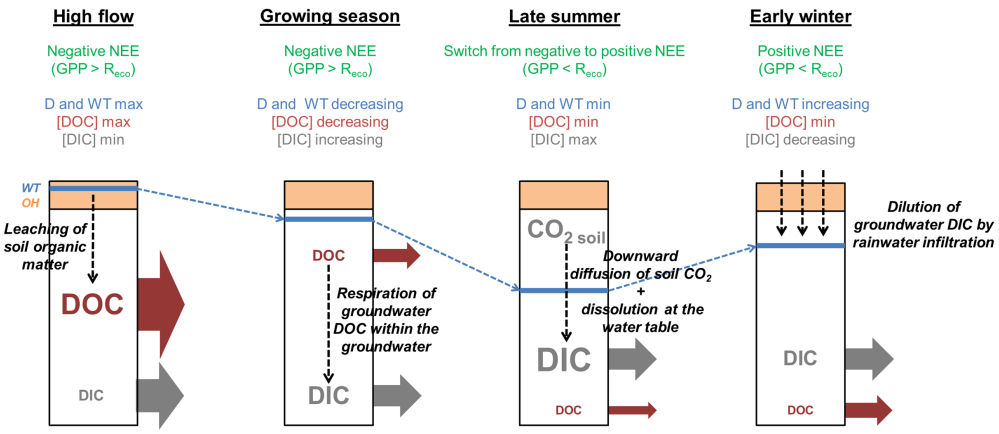

Figure 7. Conceptual model at the vegetation–soil–groundwater–stream interface in sandy ecosystems with shallow groundwater. OH, WT and *D* are the organic horizon of the soil, the water table and the drainage, respectively. Hydro-biogeochemical processes are represented by dashed arrows. Carbon exports are represented in full arrows; the thickness of the arrow indicates the magnitude of flux. High-flow periods are in January–March 2014 and February–March 2015, growing season in April–August 2014 and April–August 2015, late summer in September–October 2014 and September–October 2015, and early winter in November 2014–January 2015 and November–December 2015.

study site, the fraction of groundwater DOC that predominates at a low water table was probably more recalcitrant, more stabilized and more aged than during high flow. Indeed, in small forested watersheds, the ^{14}C age of groundwater DOC generally varies from old DOC at base flow to relatively modern DOC during high flow (Schiff et al., 1997).

In the podzol soils of the Landes de Gascogne, the saturation of the superficial organic-rich horizon of the soil was necessary to generate very high DOC concentrations in the groundwater (Figs. 4–5, 7). This suggests changes in the chemical conditions that altered the DOC retention capacity of the soil. In temperate forested ecosystems, leaching of DOC from subsoils is generally controlled by retention in the mineral B horizon of the soil with a high content of extractable aluminum and iron oxides (Kindler et al., 2011; Michalzik et al., 2001). In sandy podzols that contain almost no clay minerals (Augusto et al., 2010), DOC retention in soil is mainly controlled by organometallic complex (Lundström et al., 2000; Sauer et al., 2007). These Al–Fe oxides are considered to be the most important sorbents for dissolved organic matter in soils (Kaiser et al., 1996). In podzols such as our study site, the content in Al–Fe oxides, and their degree of complexation by soil organic matter increases with depth (Achat et al., 2011; Ferro-Vázquez et al., 2014). When the water table rises and reaches the organic-rich horizon of the soil, reducing conditions in the saturated soil will prevail. Indeed, we observed anoxic conditions in groundwater all year round at the Bilos site (data not shown). Under such reducing conditions in the saturated soil, dissolution of Fe oxides can occur, limiting the sorptive retention of DOC (Camino-Serrano et al., 2014; Fang et al., 2016; Hagedorn et al., 2000). DOC is then released to groundwater, transported downward, partly retained in the mineral horizon of the soil and exported to streams. During these high-flow periods, groundwater DOC peaked at a significantly higher value at the mesophyllous to wet Landes station (Bilos) than at the mesophyllous Landes (piezometer 3) and at the dry Landes (piezometer 2) (Table 4). This is a consequence of the water table depth and amplitude and the different carbon content in the superficial layers of the soil (Fig. 4). We calculated a stock of soil organic carbon in the 0–60 cm layer of 9.7 kg m^{-2} at the Bilos plot (Pierre Trichet and Denis Loustau, personal communication, 2014) whereas the stocks of DOC and DIC in Bilos groundwater were, on a yearly average, 0.03 and 0.06 kg m^{-2}, respectively (Fig. 6). As dissolved carbon in groundwater represents approximately 1 % of the soil carbon, only a small part of the soil organic carbon content is leached into groundwater and potentially exported to streams.

During the 3 months (March–May 2014) following the flood peak of 2014, DOC concentrations and stocks in Bilos groundwater decreased regularly in parallel with an increase in DIC concentrations and stocks in groundwater (Figs. 5–6). The DOC degradation and DIC accumulation rates in Bilos groundwater were very similar and were estimated at approximately 60 mmol m^{-2} day^{-1}, or 6.5 mmol m^{-3} day^{-1}. This DOC degradation occurred during decreasing water table periods, although these periods are characterized by moderate groundwater temperature (< 13 °C). Moreover, this DOC degradation rate is consistent with findings of Craft et al. (2002), who reported respiration rates within the range of 3–100 mmol m^{-3} day^{-1} within a floodplain aquifer of a large gravel-bed river in northwestern Montana in the US. Similarly, in a semiarid mountain catchment in New Mexico, Baker et al. (2000) also observed that groundwater DOC peaked during periods of high flow and resulted in higher

rates of heterotrophic metabolism, presumably because of the supply of labile DOC via more intense hydrologic connections between the soil and the groundwater. The bioavailability of groundwater DOC is related to the content of compounds of low molecular weight, such as amino acids or carbohydrates, and compounds of high molecular weight such as fulvic or humic acids are more recalcitrant to decomposition by microbes. Our results suggest that DOC degradation within the groundwater occurred the following months after the mobilization of biodegradable DOC during a high water table.

The increase in DIC concentrations in groundwater during late summer of 2014 (September–October 2014) was due to another process, this time not associated with any DOC degradation in groundwater (Fig. 5b–c). At our study site, the late summer period, when the forest ecosystem is a net source of CO_2 for the atmosphere (positive NEE), also corresponds to a maximum in CO_2 concentration in groundwater (Figs. 2b, 5b) and thus a maximum contribution of soil respiration to groundwater DIC. Transfer of CO_2 from soil air to groundwater requires input of fluid, i.e., gas or water (Tsypin and Macpherson, 2012). Typical pathways are downward CO_2 transport from soil in the dissolved (Kessler and Harvey, 2001) or gaseous form (Appelo and Postma, 2005), upward flux of deep CO_2 of various origins through gas vents (Chiodini et al., 1999) or leakage from adjacent aquifers. At our study site there is no evidence of a deep CO_2 source or leakage from adjacent aquifers (Bertran et al., 2011). In addition, during late dry summer, no rainy events occurred (Fig. 2c), and the high temperatures observed during this period are favorable for a high production of gaseous CO_2 in the unsaturated region of the soil, which follows the Arrhenius equation (Lloyd and Taylor, 1994; Reth et al., 2005). During high temperature periods in summer, the amount of CO_2 in equilibrium with groundwater lower than in soil upper horizons favored a downward flux of gaseous CO_2 (Tsypin and Macpherson, 2012), which suggests that soil CO_2 must have been transported to groundwater in gaseous form by simple downward diffusion (Fig. 7). In a North American tallgrass prairie resting on limestone, downward movement of CO_2 gas followed by equilibration with groundwater at the water table was favorable during a drought period, whereas transport of soil CO_2 in the dissolved form with diffuse flow of recharge water was the most effective during wet periods (Tsypin and Macpherson, 2012). In temperate forested landscapes, other authors noticed that during dry periods, a strong reduction in soil CO_2 flux to the atmosphere (upward diffusion) is associated with a decline in soil water content that stresses roots and microorganisms (Davidson et al., 1998; Epron et al., 1999). This suggests that the peak of groundwater pCO_2 observed in October 2014 (Fig. 5b) originates from soil CO_2 that was produced before, certainly during July–August 2014 when the temperature was the highest and precipitation was sufficient to maintain a soil moisture that did not limit soil respiration (Fig. 2b–c). The lag time of 2–3 months between the peak of groundwater CO_2 and soil CO_2 has been documented by Tsypin and Macpherson (2012), who concluded that it corresponded to the travel time of soil-generated CO_2 to the water table. In the sandy podzols, during the drought period, the high porosity in the sandy soil may favor downward diffusion of CO_2 and its dissolution in groundwater. Thereafter, during the early winter period, concentrations of DIC in groundwater decreased as a consequence of dilution with rainwater with low DIC content (Fig. 7).

4.3 Carbon transfer at the groundwater–stream–atmosphere interface

In the Leyre watershed, carbon exports are influenced by the soil types, which are characterized by a different water table depth and amplitude (Fig. 4), as well as a gradient of carbon content in the different soil types (Augusto et al., 2006). However, these last parameters have a stronger effect on the spatial heterogeneity of DOC exports than DIC exports (Table 5). Indeed, drainage and DOC concentrations in groundwater have a cumulative positive effect on DOC exports (Tables 1–2, 4–5; Fig. 5b–c); in contrast, drainage and DIC concentrations in groundwater have antagonistic effects on DIC exports (Tables 1–2, 4–5; Fig. 5b–c). As a consequence, groundwater exports the majority of DOC during the 2–3 months of high flow, but approximately the same quantity of DIC is exported during periods of high flow and periods of base flow (Table 5). In addition, during the study period the discharge varied by up to 100-fold (Fig. 2a); the corresponding variations in DIC and DOC concentrations and exports from the groundwater varied up to 10-fold (Tables 4–5; Figs. 4–5). As reported in other studies (Fiedler et al., 2006; Öquist et al., 2009), carbon export rates were mainly determined by discharge, the variations in carbon concentrations and exports being relatively small compared to the flow variation. However, for the whole sampling period, the mean weighted carbon export is almost the same for both DIC ($0.9 \pm 0.5\,\mathrm{mmol\,m^{-2}\,day^{-1}}$) and DOC ($0.7 \pm 0.7\,\mathrm{mmol\,m^{-2}\,day^{-1}}$) (Table 5), and the forest ecosystem exports in total $1.6 \pm 0.9\,\mathrm{mmol\,m^{-2}\,day^{-1}}$ (equivalent to $7.0 \pm 3.9\,\mathrm{g\,C\,m^{-2}\,yr^{-1}}$), 40 % as DOC and 60 % as DIC (Table 6). This terrestrial carbon leaching from groundwater to streams is of the same order of magnitude as carbon leaching from subsoils ($11.9 \pm 5.9\,\mathrm{g\,C\,m^{-2}\,yr^{-1}}$) in five temperate forest plots across Europe (Kindler et al., 2011), in a temperate Japanese deciduous forest from soils to streams ($4.0\,\mathrm{g\,C\,m^{-2}\,yr^{-1}}$) (Shibata et al., 2005), or in European forests ($9.6 \pm 3.2\,\mathrm{g\,C\,m^{-2}\,yr^{-1}}$) (Luyssaert et al., 2010).

As in groundwater, DOC and DIC concentrations in first-order streams were significantly anticorrelated (Table 2), suggesting that dissolved carbon dynamics in streams are mostly impacted by groundwater inputs (Kawasaki et al., 2005; Öquist et al., 2009). We could observe higher DOC concentrations in streams during early winter and high-flow

periods than during growing season and late summer periods (Table 4). Increase in DOC concentrations with discharge and a high water table has been reported in the Leyre watershed (Polsenaere et al., 2013) and in many other forested catchments (Alvarez-Cobelas et al., 2012; Dawson et al., 2002; Raymond and Saiers, 2010; Striegl et al., 2005). At our study site, during periods of high flow, first-order streams exported $0.2 \pm 0.2\,\mathrm{mmol\,m^{-2}\,day^{-1}}$ to second-order streams, a flux significantly lower than DOC exports ($0.7 \pm 0.7\,\mathrm{mmol\,m^{-2}\,day^{-1}}$) from groundwater to first-order streams (Table 5). As a consequence, during the sampling period, 70 % of the groundwater DOC was either degraded or re-immobilized at the groundwater–stream interface (Table 5). Indeed, when groundwater DOC enters the superficial river network through drainage part of it might be rapidly recycled by photooxidation (Macdonald and Minor, 2013; Moody and Worrall, 2016) or by respiration within the stream (Hall et al., 2016; Roberts et al., 2007). Alternatively, DOC can be re-adsorbed on Fe or Al oxides that are particularly abundant at the riverbed oxic–anoxic interface. As a matter of fact, flocculation with Fe or Al can remove DOC from solution (Sharp et al., 2006). In contrast, DOC concentrations and exports were similar and stable in groundwater and streams during periods of base flow (Table 5). This suggests that groundwater DOC behaved conservatively during low-flow stages (Schiff et al., 1997) and that DOC in streams was more labile during high-flow stages (Aravena et al., 2004). Indeed, in a small temperate and forested catchment in Pennsylvania (US), McLaughlin and Kaplan (2013) reported an increase in concentrations of labile DOC of up to 27-fold during high-flow stages compared to base-flow conditions.

DIC concentration in streams increased during the late summer period in parallel with those in groundwater (Table 4; Fig. 5b). Indeed, concentrations of DIC show an inverse relationship with discharge in the Leyre watershed (Polsenaere et al., 2013) and in other temperate catchments (Billett et al., 2004; Dawson and Smith, 2007) as the result of dilution with rain water and a lower contribution of deep CO_2-enriched groundwater during high-flow periods. The discharge of DIC-rich groundwater supersaturated with CO_2, together with the oxidation of dissolved organic matter in surface waters, results in a large CO_2 supersaturation of rivers (Hotchkiss et al., 2015; Stets et al., 2009). The quick loss of DIC between groundwater and first-order streams is due to efficient degassing of CO_2 from headwaters (Fiedler et al., 2006; Venkiteswaran et al., 2014). This rapid degassing is also attested to by the change in the $\delta^{13}C$ signature of the DIC (Deirmendjian and Abril, 2018; Polsenaere and Abril, 2012; Venkiteswaran et al., 2014). Furthermore, the positive correlation between degassing and export of DIC (Table 2) confirms that groundwater DIC is the main source of CO_2 degassing in superficial stream waters (Hotchkiss et al., 2015; Öquist et al., 2009). Very fast degassing was confirmed by observations in spring waters that lose up to 70 % of their CO_2 a few dozen meters downstream (Deirmendjian and Abril, 2018; Öquist et al., 2009). Venkiteswaran et al. (2014) concluded that most of the stream CO_2 originating from groundwater drainage was degassed before typical in-stream sampling occurs. Throughout the sampling period degassing was, on a yearly average, approximately $0.7 \pm 0.5\,\mathrm{mmol\,m^{-2}\,day^{-1}}$ (equivalent to $3.1 \pm 2.2\,\mathrm{g\,C\,m^{-2}\,yr^{-1}}$). CO_2 degassing was higher during high-flow periods than during periods of base flow (Table 5), as a consequence of higher discharge and inputs of groundwater DIC to streams (Tables 1, 4) and higher water turbulence. As a matter of fact, degassing depends on water velocity that induces water turbulence and thus increases the gas transfer velocity (Alin et al., 2011; Raymond et al., 2012). Overall, during the whole sampling period CO_2 degassing in streams represented approximately 75 % of the DIC exported from groundwater and thus a significant part of the carbon exported from forest rapidly returns to the atmosphere in the form of CO_2 through degassing.

Leaching of terrestrial carbon from the pine forest in the Leyre watershed calculated as the DOC and DIC export per catchment area was $1.6 \pm 0.9\,\mathrm{mmol\,m^{-2}\,day^{-1}}$ (equivalent to $7.0 \pm 3.9\,\mathrm{g\,C\,m^{-2}\,yr^{-1}}$). Eddy covariance measurements at the Bilos plot (Table 3) provided a forest net uptake of atmospheric CO_2 of approximately $-90 \pm 110\,\mathrm{mmol\,m^{-2}\,day^{-1}}$ (equivalent to $390 \pm 480\,\mathrm{g\,C\,m^{-2}\,yr^{-1}}$). In the same way that groundwater DOC and DIC stocks represent a minor fraction of soil carbon, carbon leaching represents a very small (approximately 2 %) fraction of forest NEE, a conclusion consistent with other studies in temperate forest ecosystems (Kindler et al., 2011; Magin et al., 2017; Shibata et al., 2005). Such weak export of carbon from forest ecosystems, at least in temperate regions, is at odds with recent studies that attempt to integrate the contribution of inland waters in the continents' carbon budget (Ciais et al., 2013). Indeed, on the global scale, the quantity of terrestrial carbon necessary to account for the sum of CO_2 degassing from inland waters, organic carbon burial in sediments and carbon export to the ocean represents more than $2\,\mathrm{Pg\,C\,yr^{-1}}$, a number similar to the actual net land sink of atmospheric CO_2 (Ciais et al., 2013). Understanding why local and global carbon mass balances strongly diverge on the proportion of land NEE exported to aquatic systems appears to be a major challenge for the next years of research in this field.

5 Conclusion

The monitoring of DIC and DOC concentrations in groundwater and first-order streams in podzol-dominated catchment overlaid by pine forest brings new insights on the nature of processes that control carbon leaching from soils, transformation in groundwater, and export to surface waters and back to the atmosphere (Fig. 7). This terrestrial–aquatic–

atmosphere interface is believed to behave as a hotspot in the continental carbon cycle. The permeable character of the soil at the study site enables a clear temporal decomposition of processes involving carbon in groundwaters in relation with water table depth and amplitude, forest ecosystem production, and respiration. Hydrology has a strong influence on the carbon concentrations in shallow groundwater. High precipitation caused the water table to rise and saturate the topsoil, inducing a large mobilization of soil organic matter as DOC in the shallow groundwater, a process also favored by temporarily reducing conditions in the topsoil. These periods of a high water table are also associated with low DIC concentrations in groundwater caused by the groundwater dilution with rainwater. Conversely, groundwater was enriched in DIC during base-flow stages, as the result of two distinct processes. First, microbial consumption of DOC occurs within the groundwater in spring and summer, the following months after the periods of a high water table. Second, heterotrophic conditions in the forest ecosystem during late summer favor the downward diffusion of soil CO_2 to shallow groundwater.

In the absence of surface runoff, the comparison of dissolved carbon concentrations between groundwater and streams, associated with drainage data, allows us to understand and quantify the processes at the groundwater–stream–atmosphere interface. In the studied catchment, this method reveals a fast degassing of DIC as CO_2 throughout the year in first-order streams. During base-flow periods, groundwater DOC was exported conservatively to streams, probably because groundwater DOC was more recalcitrant, more stabilized and more aged during this period. However, during stages of a high water table, DOC concentrations in groundwater increased at some sites but not at others. This spatial heterogeneity of carbon export in the landscape did not fully translate in streams because of fast DOC degradation within the groundwater and/or DOC re-adsorption processes in soils close to the groundwater–streams interface.

Although spatial extrapolation of quantitative information from the plot scale to first-order streams in the watershed may have generated some uncertainty, we could make a comparison of groundwater carbon export to stream with other carbon fluxes in the landscape. Representing 2 % of the local forest NEE, DIC and DOC exports to surface waters do not seem to be a significant component of the carbon budget at our study site. More detailed work at the land–water interface is necessary in order to reconcile the contradictory findings on local and global scales on the significance of hydrological carbon export in the continental carbon budget.

Data availability. Bilos site (FR-BIL) is a station as part of the ICOS project (https://www.icos-ri.eu/). Eddy covariance, meteorological and water table depth data are measured continuously at the Bilos pine plot. These data are available upon request to Denis Loustau (denis.loustau@inra.fr). River discharge data are measured continuously by the French water survey agency (DIREN) and are available at http://www.hydro.eaufrance.fr. Carbon raw data are stored on data servers and repositories and available upon request to the corresponding author.

The Supplement related to this article is available online at https://doi.org/10.5194/bg-15-669-2018-supplement.

Competing interests. The authors declare that they have no conflict of interest.

Acknowledgements. This research is part of the CNP-Leyre project funded by the Cluster of Excellence COTE at the Université de Bordeaux (ANR-10-LABX-45). We thank Luiz Carlos Cotovicz Junior, Katixa Lajaunie-Salla, Baptiste Voltz, Gwenaëlle Chaillou and Damien Buquet (EPOC Bordeaux) for their assistance in the field. We thank Pierre Anshutz (EPOC, Bordeaux), Alain Mollier and Christian Morel (ISPA INRA) for their involvement in the CNP-Leyre project, and Céline Charbonnier for alkalinity titrations in the laboratory. Pierre Trichet (ISPA INRA) provided SOC data at the Bilos site.

Edited by: Nobuhito Ohte
Reviewed by: Masanori Katsuyama and one anonymous referee

References

Abril, G., Bouillon, S., Darchambeau, F., Teodoru, C. R., Marwick, T. R., Tamooh, F., Ochieng Omengo, F., Geeraert, N., Deirmendjian, L., Polsenaere, P., and Borges, A. V.: Technical Note: Large overestimation of pCO_2 calculated from pH and alkalinity in acidic, organic-rich freshwaters, Biogeosciences, 12, 67–78, https://doi.org/10.5194/bg-12-67-2015, 2015.

Achat, D. L., Bakker, M. R., and Trichet, P.: Rooting patterns and fine root biomass of Pinus pinaster assessed by trench wall and core methods, J. Forest Res., 13, 165–175, 2008.

Achat, D. L., Augusto, L., Morel, C., and Bakker, M. R.: Predicting available phosphate ions from physical–chemical soil properties in acidic sandy soils under pine forests, J. Soil. Sediment, 11, 452–466, 2011.

Ahuja, L. R., Ma, L., and Green, T. R.: Effective soil properties of heterogeneous areas for modeling infiltration and redistribution, Soil Sci. Soc. Am. J., 74, 1469–1482, 2010.

Alin, S. R., de Fátima F. L. Rasera, M., Salimon, C. I., Richey, J. E., Holtgrieve, G. W., Krusche, A. V., and Snidvongs, A.: Physical controls on carbon dioxide transfer velocity and flux in low-gradient river systems and implications for regional carbon budgets, J. Geophys. Res.-Biogeo., 116, G01009, https://doi.org/10.1029/2010JG001398, 2011.

Alley, W. M., Healy, R. W., LaBaugh, J. W., and Reilly, T. E.: Flow and storage in groundwater systems, Science, 296, 1985–1990, 2002.

Alvarez-Cobelas, M., Angeler, D. G., Sánchez-Carrillo, S., and Almendros, G.: A worldwide view of organic carbon export from catchments, Biogeochemistry, 107, 275–293, 2012.

Appelo, C. A. J. and Postma, D.: Geochemistry, Groundwater, and Pollution, second ed., Balkema, Rotterdam, the Netherlands, 2005.

Aravena, R., Wassenaar, L. I., and Spiker, E. C.: Chemical and carbon isotopic composition of dissolved organic carbon in a regional confined methanogenic aquifer, Isot. Environ. Healt. S., 40, 103–114, 2004.

Artinger, R., Buckau, G., Geyer, S., Fritz, P., Wolf, M., and Kim, J. I.: Characterization of groundwater humic substances: influence of sedimentary organic carbon, Appl. Geochem. 15, 97–116, 2000.

Atkins, M. L., Santos, I. R., Ruiz-Halpern, S., and Maher, D. T.: Carbon dioxide dynamics driven by groundwater discharge in a coastal floodplain creek, J. Hydrol., 493, 30–42, 2013.

Aubinet, M., Grelle, A., Ibrom, A., Rannik, Ü., Moncrieff, J., Foken, T., Kowalski, A. S., Martin, P. H., Berbigier, P., Bernhofer, C., Clement, R., Elbers, A., Granier, A., Grunwald, T., Morgensterm, K., Pilegaard, C., Rebmann, C., Snijders, W., Valentini, R., and Vesala, T.: Estimates of the annual net carbon and water exchange of forests: the EUROFLUX methodology, Adv. Ecol. Res., 30, 113–175, 1999.

Augusto, L., Badeau, V., Arrouays, D., Trichet, P., Flot, J. L., Jolivet, C., and Merzeau, D.: Caractérisation physico-chimique des sols à l'échelle d'une région naturelle à partir d'une compilation de données. Exemple des sols du massif forestier landais, Etude et gestion des sols, 13, 7–22, 2006.

Augusto, L., Bakker, M. R., Morel, C., Meredieu, C., Trichet, P., Badeau, V., Arrouays, D., Plassard, C., Achat, D.L., Gallet-Budynek, A., Merzeau, D., Canteloup, D., Najar, M., and Ranger, J.: Is "grey literature" a reliable source of data to characterize soils at the scale of a region? A case study in a maritime pine forest in southwestern France, Eur. J. Soil Sci., 61, 807–822, https://doi.org/10.1111/j.1365-2389.2010.01286.x, 2010.

Baker, M. A., Valett, H. M., and Dahm, C. N.: Organic carbon supply and metabolism in a shallow groundwater ecosystem, Ecology, 81, 3133–3148, 2000.

Bakker, M. R., Augusto, L., and Achat, D. L.: Fine root distribution of trees and understory in mature stands of maritime pine (Pinus pinaster) on dry and humid sites, Plant Soil, 286, 37–51, 2006.

Bakker, M. R., Jolicoeur, E., Trichet, P., Augusto, L., Plassard, C., Guinberteau, J., and Loustau, D.: Adaptation of fine roots to annual fertilization and irrigation in a 13-year-old Pinus pinaster stand, Tree Physiol., 29, 229–238, 2009.

Battin, T. J., Luyssaert, S., Kaplan, L. A., Aufdenkampe, A. K., Richter, A., and Tranvik, L. J.: The boundless carbon cycle, Nat. Geosci., 2, 598–600, 2009.

Bertran, P., Allenet, G., Gé, T., Naughton, F., Poirier, P., and Goñi, M. F. S.: Coversand and Pleistocene palaeosols in the Landes region, southwestern France, J. Quaternary Sci., 24, 259–269, 2009.

Bertran, P., Bateman, M. D., Hernandez, M., Mercier, N., Millet, D., Sitzia, L., and Tastet, J.-P.: Inland aeolian deposits of south-west France: facies, stratigraphy and chronology, J. Quaternary Sci., 26, 374–388, 2011.

Billett, M. F., Palmer, S. M., Hope, D., Deacon, C., Storeton-West, R., Hargreaves, K. J., Flechard, C., and Fowler, D.: Linking land-atmosphere-stream carbon fluxes in a lowland peatland system, Global Biogeochem. Cy., 18, GB1024, https://doi.org/10.1029/2003GB002058, 2004.

Bolan, N. S., Adriano, D. C., Kunhikrishnan, A., James, T., McDowell, R., and Senesi, N.: Dissolved organic matter: biogeochemistry, dynamics, and environmental significance in soils, Adv. Agron., 110, 1–75, https://doi.org/10.1016/B978-0-12-385531-2.00001-3, 2011.

Bosch, J. M. and Hewlett, J. D.: A review of catchment experiments to determine the effect of vegetation changes on water yield and evapotranspiration, J. Hydrol., 55, 3–23, 1982.

Butman, D. and Raymond, P. A.: Significant efflux of carbon dioxide from streams and rivers in the United States, Nat. Geosci., 4, 839–842, https://doi.org/10.1038/ngeo1294, 2011.

Camino-Serrano, M., Gielen, B., Luyssaert, S., Ciais, P., Vicca, S., Guenet, B., Vos, B. D., Cools, N., Ahrens, B., Altaf Arain, M., Borken, W., Clarke, N., Clarkson, B., Cummins, T., Don, A., Graf Pannatier, E., Laudon, H., Moore, T., Nieminen, T., Nilsson, M. B., Peichi, M., Schwendenmann, L., Siemens, J., and Janssens, I. A.: Linking variability in soil solution dissolved organic carbon to climate, soil type, and vegetation type, Global Biogeochem. Cy., 28, 497–509, 2014.

Chiodini, G., Frondini, F., Kerrick, D. M., Rogie, J., Parello, F., Peruzzi, L., and Zanzari, A. R.: Quantification of deep CO_2 fluxes from Central Italy. Examples of carbon balance for regional aquifers and of soil diffuse degassing, Chem. Geol., 159, 205–222, 1999.

Ciais, P., Sabine, C., Bala, G., Bopp, L., Brovkin, V., Canadell, J., Chhabra, A., DeFries, R., Galloway, J., Heimann, M., Jones, C., Le Quéré, C., Myeni, R., Piao, S., and Thornton, P.: Carbon and other biogeochemical cycles, in: Climate Change 2013: The Physical Science Basis. Contribution of Working Group I to the Fifth Assessment Report of the Intergovernmental Panel on Climate Change. Cambridge University Press, Cambridge, UK and New York, NY, USA., 465–570, 2013.

Cole, J. J., Prairie, Y. T., Caraco, N. F., McDowell, W. H., Tranvik, L. J., Striegl, R. G., Duarte, C. M., Kortelainen, P., Downing, J. A., Middelburg, J. J., and Melack, J.: Plumbing the Global Carbon Cycle: Integrating Inland Waters into the Terrestrial Carbon Budget, Ecosystems, 10, 171–184, https://doi.org/10.1007/s10021-006-9013-8, 2007.

Corbier, P., Karnay, G., Bourgine, B., and Saltel, M.: Gestion des eaux souterraines en région Aquitaine – Reconnaissance des potentialités aquiferes du Mio-Plio-Quaternaire des Landes de Gascogne et du Médoc en relation avec les SAGE, Module 7 (No. 57813), BRGM, Orléans, France, 187 pp., 2010.

Craft, J. A., Stanford, J. A., and Pusch, M.: Microbial respiration within a floodplain aquifer of a large gravel-bed river, Freshwater Biol., 47, 251–261, 2002.

Datry, T., Malard, F., and Gibert, J.: Dynamics of solutes and dissolved oxygen in shallow urban groundwater below a stormwater infiltration basin, Sci. Total Environ., 329, 215–229, 2004.

David, T. S., Pinto, C. A., Nadezhdina, N., Kurz-Besson, C., Henriques, M. O., Quilhó, T., Cermak, J., Chaves, M. M., Pereira, J. S., and David, J. S.: Root functioning, tree water use and hydraulic redistribution in Quercus suber trees: a modeling approach based on root sap flow, Forest Ecol. Manag., 307, 136–146, 2013.

Davidson, E., Belk, E., and Boone, R. D.: Soil water content and temperature as independent or confounded factors controlling soil respiration in a temperate mixed hardwood forest, Glob. Change Biol., 4, 217–227, 1998.

Dawson, J. J. and Smith, P.: Carbon losses from soil and its consequences for land-use management, Sci. Total Environ., 382, 165–190, 2007.

Dawson, J. J. C., Billett, M. F., Neal, C., and Hill, S.: A comparison of particulate, dissolved and gaseous carbon in two contrasting upland streams in the UK, J. Hydrol., 257, 226–246, 2002.

Deirmendjian, L. and Abril, G.: Carbon dioxide degassing at the groundwater-stream-atmosphere interface: isotopic equilibration and hydrological mass balance in a sandy watershed, J. Hydrol., https://doi.org/10.1016/j.jhydrol.2018.01.003, in press, 2018.

Del Castillo, J., Comas, C., Voltas, J., and Ferrio, J. P.: Dynamics of competition over water in a mixed oak-pine Mediterranean forest: spatio-temporal and physiological components, Forest Ecol. Manag., 382, 214–224, 2016.

Domec, J.-C., King, J. S., Noormets, A., Treasure, E., Gavazzi, M. J., Sun, G., and McNulty, S. G.: Hydraulic redistribution of soil water by roots affects whole-stand evapotranspiration and net ecosystem carbon exchange, New Phytol. 187, 171–183, 2010.

Einarsdottir, K., Wallin, M. B., and Sobek, S.. High terrestrial carbon load via groundwater to a boreal lake dominated by surface water inflow, J. Geophys. Res.-Biogeo., 122, 15–29, 2017.

Epron, D., Farque, L., Lucot, É., and Badot, P.-M.: Soil CO_2 efflux in a beech forest: dependence on soil temperature and soil water content, Ann. For. Sci., 56, 221–226, 1999.

Evans, C. D., Monteith, D. T., and Cooper, D. M.: Long-term increases in surface water dissolved organic carbon: observations, possible causes and environmental impacts, Environ. Pollut., 137, 55–71, 2005.

Fang, W., Wei, Y., Liu, J., Kosson, D. S., van der Sloot, H. A., and Zhang, P.: Effects of aerobic and anaerobic biological processes on leaching of heavy metals from soil amended with sewage sludge compost, Waste Manage., 58, 324–334, 2016.

Ferro-Vázquez, C., Nóvoa-Muñoz, J. C., Costa-Casais, M., Klaminder, J., and Martínez-Cortizas, A.: Metal and organic matter immobilization in temperate podzols: A high resolution study, Geoderma, 217–218, 225–234, https://doi.org/10.1016/j.geoderma.2013.10.006, 2014.

Fiedler, S., Höll, B. S., and Jungkunst, H. F.: Discovering the importance of lateral CO_2 transport from a temperate spruce forest, Sci. Total Environ., 368, 909–915, 2006.

Foken, T. and Wichura, B.: Tools for quality assessment of surface-based flux measurements, Agr. Forest Meteorol., 78, 83–105, 1996.

Frankignoulle, M. and Borges, A. V.. Direct and Indirect pCO_2 Measurements in a Wide Range of pCO_2 and Salinity Values (The Scheldt Estuary), Aquat. Geochem., 7, 267–273, https://doi.org/10.1023/A:1015251010481, 2001.

Goldscheider, N., Hunkeler, D., and Rossi, P.: Microbial biocenoses in pristine aquifers and an assessment of investigative methods, Hydrogeol. J., 14, 926–941, 2006.

Govind, A., Bonnefond, J.-M., Kumari, J., Moisy, C., Loustau, D., and Wigneron, J.-P.: Modeling the ecohydrological processes in the Landes de Gascogne, SW France, in: 2012 IEEE 4th International Symposium on Plant Growth Modeling, Simulation, Visualization and Applications, 31 October–3 November 2012, Shangai, China, 133–140, https://doi.org/10.1109/PMA.2012.6524824, 2012.

Gran, G.: Determination of the equivalence point in potentiometric titrations of seawater with hydrochloric acid, Oceanol. Acta, 5, 209–218, 1952.

Hagerdon, F., Schleppi, P., Waldner, P., and Fluhler, H.: Export of dissolved organic carbon and nitrogen from Gleysol dominated catchments–the significance of water flow paths, Biogeochemistry, 50, 137–161, 2000.

Hall Jr., R. O., Tank, J. L., Baker, M. A., Rosi-Marshall, E. J., and Hotchkiss, E. R.: Metabolism, gas exchange, and carbon spiraling in rivers, Ecosystems, 19, 73–86, 2016.

Heimann, M. and Reichstein, M.: Terrestrial ecosystem carbon dynamics and climate feedbacks, Nature, 451, 289–292, 2008.

Hope, D., Billett, M. F., and Cresser, M. S.: A review of the export of carbon in river water: fluxes and processes, Environ. Pollut., 84, 301–324, 1994.

Hotchkiss, E. R., Hall Jr., R. O., Sponseller, R. A., Butman, D., Klaminder, J., Laudon, H., Rosvall, M., and Karlsson, J.: Sources of and processes controlling CO_2 emissions change with the size of streams and rivers, Nat. Geosci., 8, 696–699, 2015.

Ibrom, A., Dellwik, E., Flyvbjerg, H., Jensen, N. O., and Pilegaard, K.: Strong low-pass filtering effects on water vapour flux measurements with closed-path eddy correlation systems, Agr. Forest Meteorol., 147, 140–156, 2007.

Johnson, M. S., Lehmann, J., Couto, E. G., Novaes Filho, J. P., and Riha, S. J.: DOC and DIC in flowpaths of Amazonian headwater catchments with hydrologically contrasting soils, Biogeochemistry, 81, 45–57, 2006.

Johnson, M. S., Lehmann, J., Riha, S. J., Krusche, A. V., Richey, J. E., Ometto, J. P. H., and Couto, E. G.: CO_2 efflux from Amazonian headwater streams represents a significant fate for deep soil respiration, Geophys. Res. Lett., 35, L17401, https://doi.org/10.1029/2008GL034619, 2008.

Jolivet, C., Augusto, L., Trichet, P., and Arrouays, D.: Forest soils in the Gascony Landes Region: formation, history, properties and spatial varaibility, Revue forestière française, 59, 7–30, https://doi.org/10.4267/2042/8480, 2007.

Jones, J. B. and Mulholland, P. J.: Carbon dioxide variation in a hardwood forest stream: an integrative measure of whole catchment soil respiration, Ecosystems, 1, 183–196, 1998.

Jonsson, A., Algesten, G., Bergström, A.-K., Bishop, K., Sobek, S., Tranvik, L. J., and Jansson, M.: Integrating aquatic carbon fluxes in a boreal catchment carbon budget, J. Hydrol., 334, 141–150, 2007.

Kaimal, J. C. and Finnigan, J. J.: Atmospheric boundary layer flows: their structure and measurement, Oxford University Press, New York, USA, 1994.

Kaiser, K. and Guggenberger, G.: The role of DOM sorption to mineral surfaces in the preservation of organic matter in soils, Org. Geochem., 31, 711–725, 2000.

Kaiser, K., Guggenberger, G., and Zech, W.: Sorption of DOM and DOM fractions to forest soils, Geoderma, 74, 281–303, 1996.

Kalbitz, K. and Kaiser, K.: Contribution of dissolved organic matter to carbon storage in forest mineral soils, J. Plant Nutr. Soil Sc., 171, 52–60, 2008.

Kalbitz, K., Solinger, S., Park, J.-H., Michalzik, B., and Matzner, E.: Controls on the dynamics of dissolved organic matter in soils: a review, Soil Sci. 165, 277–304, 2000.

Kawasaki, M., Ohte, N., and Katsuyama, M.: Biogeochemical and hydrological controls on carbon export from a forested catchment in central Japan, Ecol. Res., 20, 347–358, 2005.

Kessler, T. J. and Harvey, C. F.: The global flux of carbon dioxide into groundwater, Geophys. Res. Lett., 28, 279–282, 2001.

Kindler, R., Siemens, J. A. N., Kaiser, K., Walmsley, D. C., Bernhofer, C., Buchmann, N., Cellier, P., Eugster, W., Gleixner, G., Grünwald, T., Heim, A., Ibrom, A., Jones, S. K., Jones, M., Klumpp, K., Kutsch, W., Larsen, K. S., Lehuger, S., Loubet, B., Mckenzie, R., Moors, E., Osborne, B., Pilegaard, K., Rebmann, C., Saunders, M., Schmidt, M. W. I., Schrumpf, M., Seyfferth, J., Skiba, U., Soussana, J.-F., Sutton, M. A., Tefs, C., Vowinckel, B., Zeeman, M. J., and Kaupenjohann, M.: Dissolved carbon leaching from soil is a crucial component of the net ecosystem carbon balance, Glob. Change Biol., 17, 1167–1185, 2011.

Klein, T., Rotenberg, E., Cohen-Hilaleh, E., Raz-Yaseef, N., Tatarinov, F., Preisler, Y., Ogée, J., Cohen, S., and Yakir, D.: Quantifying transpirable soil water and its relations to tree water use dynamics in a water-limited pine forest, Ecohydrology, 7, 409–419, 2014.

Kokic, J., Wallin, M. B., Chmiel, H. E., Denfeld, B. A., and Sobek, S.: Carbon dioxide evasion from headwater systems strongly contributes to the total export of carbon from a small boreal lake catchment, J. Geophys. Res.-Biogeo., 120, 13–28, https://doi.org/10.1002/2014JG002706, 2015.

Kowalski, S., Sartore, M., Burlett, R., Berbigier, P., and Loustau, D.: The annual carbon budget of a French pine forest (Pinus pinaster) following harvest, Glob. Change Biol., 9, 1051–1065, 2003.

Legigan, P.: L'élaboration de la formation du sable des Landes, dépôt résiduel de l'environnement sédimentaire pliocène-pléïstocène centre aquitain, Thèse de Doctorat d'Etat no. 642, Université de Bordeaux I, Bordeaux, France, 429 pp., 1979.

Leith, F. I., Dinsmore, K. J., Wallin, M. B., Billett, M. F., Heal, K. V., Laudon, H., Öquist, M. G., and Bishop, K.: Carbon dioxide transport across the hillslope–riparian–stream continuum in a boreal headwater catchment, Biogeosciences, 12, 1881–1892, https://doi.org/10.5194/bg-12-1881-2015, 2015.

Lewis, E., Wallace, D., and Allison, L. J.: Program developed for CO_2 system calculations, ORNL/CDIAC-105, Carbon Dioxide Information Analysis Center, Oak Ridge National Laboratory, U.S. Department of Energy, Oak Ridge, Tennessee, USA, 1998.

Lloyd, J. and Taylor, J. A.: On the temperature dependence of soil respiration, Funct. Ecol., 8, 315–323, 1994.

Loustau, D. and Guillot, M.: Impact écologique de la tempête et conséquences sur les cycles de l'eau et du carbone, Innovations Agronomiques, 6, 1–6, 2009.

Loustau, D., Granier, A., and El Hadj Moussa, F.: Seasonal variations of sap flow in a maritime pine standard [hydraulic conductance, stomatal conductance], Annales des Sciences Forestieres (France), 21, 599–618, 1990.

Lundström, U., Van Breemen, N., Bain, D. C., Van Hees, P. A. W., Giesler, R., Gustafsson, J. P., Ilvesniemi, H., Karltun, E., Melkerud, P.-A., Olsson, M., Riise, G., Wahlberg, O., Bergelin, A., Bishop, K., Finlay, R., Jongmans, A. G., Magnusson, T., Mannerkoski, H., Nordgren, A., Nyberg, L., Starr, M., and Tau Strand, L.: Advances in understanding the podzolization process resulting from a multidisciplinary study of three coniferous forest soils in the Nordic Countries, Geoderma, 94, 335–353, 2000.

Luyssaert, S., Ciais, P., Piao, S. L., Schulze, E.-D., Jung, M., Zaehle, S., Schelhaas, M. J., Reichstein, M., Churkina, G., Papale, D., Abril, G., Beer, C., Grace, J., Loustau, D., Matteucci, G., Magnani, F., Nabuurs, G. J., Verbeeck, H., Sulkava, M., Van Der Werf, G. R., Janssens, I. A., and Members Of The Carboeurope-Ip Synthesis Team: The European carbon balance. Part 3: forests, Glob. Change Biol., 16, 1429–1450, 2010.

Macdonald, M. J. and Minor, E. C.: Photochemical degradation of dissolved organic matter from streams in the western Lake Superior watershed, Aquat. Sci., 75, 509–522, 2013.

Magin, K., Somlai-Haase, C., Schäfer, R. B., and Lorke, A.: Regional-scale lateral carbon transport and CO_2 evasion in temperate stream catchments, Biogeosciences, 14, 5003–5014, https://doi.org/10.5194/bg-14-5003-2017, 2017.

McClain, M. E., Boyer, E. W., Dent, C. L., Gergel, S. E., Grimm, N. B., Groffman, P. M., Hart, S. C., Harvey, J. W., Johnston, C. A., Mayorga, E., McDowell, W. H., and Pinay, G.: Biogeochemical hot spots and hot moments at the interface of terrestrial and aquatic ecosystems, Ecosystems, 6, 301–312, 2003.

McLaughlin, C. and Kaplan, L. A.: Biological lability of dissolved organic carbon in stream water and contributing terrestrial sources, Freshw. Sci., 32, 1219–1230, 2013.

Mendes, M. P., Ribeiro, L., David, T. S., and Costa, A.: How dependent are cork oak (Quercus suber L.) woodlands on groundwater? A case study in southwestern Portugal, Forest Ecol. Manag., 378, 122–130, 2016.

Michalzik, B., Kalbitz, K., Park, J.-H., Solinger, S., and Matzner, E.: Fluxes and concentrations of dissolved organic carbon and nitrogen – a synthesis for temperate forests, Biogeochemistry, 52, 173–205, 2001.

Millero, F. J.: The thermodynamics of the carbonate system in seawater, Geochim. Cosmochim. Ac., 43, 1651–1661, 1979.

Moody, C. S. and Worrall, F.: Sub-daily rates of degradation of fluvial carbon from a peat headwater stream, Aquat. Sci., 78, 419–431, 2016.

Moreaux, V., Lamaud, É., Bosc, A., Bonnefond, J.-M., Medlyn, B. E., and Loustau, D.: Paired comparison of water, energy and carbon exchanges over two young maritime pine stands (Pinus pinaster Ait.): effects of thinning and weeding in the early stage of tree growth, Tree Physiol., 31, 903–921, https://doi.org/10.1093/treephys/tpr048, 2011.

Oki, T. and Kanae, S.: Global hydrological cycles and world water resources, Science, 313, 1068–1072, 2006.

Olefeldt, D., Roulet, N., Giesler, R., and Persson, A.: Total waterborne carbon export and DOC composition from ten nested subarctic peatland catchments—importance of peatland cover, groundwater influence, and inter-annual variability of precipitation patterns, Hydrol. Process., 27, 2280–2294, 2013.

Öquist, M. G., Wallin, M., Seibert, J., Bishop, K., and Laudon, H.: Dissolved inorganic carbon export across the soil/stream interface and its fate in a boreal headwater stream, Environ. Sci. Technol., 43, 7364–7369, 2009.

Pabich, W. J., Valiela, I., and Hemond, H. F.: Relationship between DOC concentration and vadose zone thickness and depth below water table in groundwater of Cape Cod, USA, Biogeochemistry, 55, 247–268, 2001.

Polsenaere, P. and Abril, G.: Modelling CO_2 degassing from small acidic rivers using water pCO_2, DIC and

δ13C-DIC data, Geochim. Cosmochim. Ac., 91, 220–239, https://doi.org/10.1016/j.gca.2012.05.030, 2012.

Polsenaere, P., Savoye, N., Etcheber, H., Canton, M., Poirier, D., Bouillon, S., and Abril, G.: Export and degassing of terrestrial carbon through watercourses draining a temperate podzolized catchment, Aquat. Sci., 75, 299–319, 2013.

Querejeta, J. I., Roldán, A., Albaladejo, J., and Castillo, V.: Soil water availability improved by site preparation in a Pinus halepensis afforestation under semiarid climate, Forest Ecol. Manag., 149, 115–128, 2001.

Raymond, P. A. and Saiers, J. E.: Event controlled DOC export from forested watersheds, Biogeochemistry, 100, 197–209, 2010.

Raymond, P. A., Zappa, C. J., Butman, D., Bott, T. L., Potter, J., Mulholland, P., Laursen, A. E., McDowell, W. H., and Newbold, D.: Scaling the gas transfer velocity and hydraulic geometry in streams and small rivers, Limnol. Oceanogr.: Fluids and Environments, 2, 41–53, 2012.

Raymond, P. A., Hartmann, J., Lauerwald, R., Sobek, S., McDonald, C., Hoover, M., Butman, D., Striegl, R., Mayorga, E., Humborg, C., Kortelainen, P., Dürr, H., Meybeck, M., Ciais, P., and Guth, P.: Global carbon dioxide emissions from inland waters, Nature, 503, 355–359, https://doi.org/10.1038/nature12760, 2013.

Regnier, P., Friedlingstein, P., Ciais, P., Mackenzie, F. T., Gruber, N., Janssens, I. A., Laruelle, G. G., Lauerwald, R., Luyssaert, S., Andersson, A. J., Arndt, S., Arnosti, C., Borges, A., Dale, A., Gallego-Sala, A., Goddéris, Y., Goosens, N., Hartmann, J., Heinze, C., Ilyina, T., Joos, F., LaRowe, D., Leifeld, J., Meysman, J., Munhoven, G., Raymond, P., Spahni, R., Suntharalingam, P., and Thullner, M.: Anthropogenic perturbation of the carbon fluxes from land to ocean, Nat. Geosci., 6, 597–607, 2013.

Reichstein, M., Falge, E., Baldocchi, D., Papale, D., Aubinet, M., Berbigier, P., Bernhofer, C., Buchmann, N., Gilmanov, T., Granier, A., Grünwald, T., Havránková, K., Ilvesniemi, H., Janous, D., Knohl, A., Laurila, T., Lohila, A., Loustau, D., Matteucci, G., Meyers, T., Miglietta, F., Ourcival, J.-M., Pumpanen, J., Rambal, S., Rotenberg, E., Sanz, M., Tenhunen, J., Seufert, G., Vaccari, F., Vesala, T., Yakir, D., and Valentini, R.: On the separation of net ecosystem exchange into assimilation and ecosystem respiration: review and improved algorithm, Glob. Change Biol., 11, 1424–1439, 2005.

Reth, S., Reichstein, M., and Falge, E.: The effect of soil water content, soil temperature, soil pH-value and the root mass on soil CO_2 efflux – A modified model, Plant Soil, 268, 21–33, 2005.

Roberts, B. J., Mulholland, P. J., and Hill, W. R.: Multiple scales of temporal variability in ecosystem metabolism rates: results from 2 years of continuous monitoring in a forested headwater stream, Ecosystems, 10, 588–606, 2007.

Sadat-Noori, M., Maher, D. T., and Santos, I. R.: Groundwater discharge as a source of dissolved carbon and greenhouse gases in a subtropical estuary, Estuar. Coast., 39, 639–656, 2016.

Sanderman, J. and Amundson, R.: A comparative study of dissolved organic carbon transport and stabilization in California forest and grassland soils, Biogeochemistry, 92, 41–59, 2009.

Santos, I. R., Maher, D. T., and Eyre, B. D.: Coupling automated radon and carbon dioxide measurements in coastal waters, Environ. Sci. Technol., 46, 7685–7691, 2012.

Sauer, D., Sponagel, H., Sommer, M., Giani, L., Jahn, R., and Stahr, K.: Podzol: Soil of the year 2007. A review on its genesis, occurrence, and functions, J. Plant Nutr. Soil Sc., 170, 581–597, 2007.

Schiff, S. L., Aravena, R., Trumbore, S. E., Hinton, M. J., Elgood, R., and Dillon, P. J.: Export of DOC from forested catchments on the Precambrian Shield of Central Ontario: clues from ^{13}C and ^{14}C, Biogeochemistry, 36, 43–65, 1997.

Schimel, D. S., House, J. I., Hibbard, K. A., Bousquet, P., Ciais, P., Peylin, P., Braswell, B. H., Apps, M. J., Baker, D., and Bondeau, A.: Recent patterns and mechanisms of carbon exchange by terrestrial ecosystems, Nature, 414, 169–172, 2001.

Sharp, E. L., Jarvis, P., Parsons, S. A., and Jefferson, B.: Impact of fractional character on the coagulation of NOM, Colloid. Surface. A, 286, 104–111, 2006.

Shen, Y., Chapelle, F. H., Strom, E. W., and Benner, R.: Origins and bioavailability of dissolved organic matter in groundwater, Biogeochemistry, 122, 61–78, 2015.

Shibata, H., Mitsuhashi, H., Miyake, Y., and Nakano, S.: Dissolved and particulate carbon dynamics in a cool-temperate forested basin in northern Japan, Hydrol. Process., 15, 1817–1828, 2001.

Shibata, H., Hiura, T., Tanaka, Y., Takagi, K., and Koike, T.: Carbon cycling and budget in a forested basin of southwestern Hokkaido, northern Japan, Ecol. Res., 20, 325–331, 2005.

Stets, E. G., Striegl, R. G., Aiken, G. R., Rosenberry, D. O., and Winter, T. C.: Hydrologic support of carbon dioxide flux revealed by whole-lake carbon budgets, J. Geophys. Res.-Biogeo., 114, G01008, https://doi.org/10.1029/2008JG000783, 2009.

Striegl, R. G., Aiken, G. R., Dornblaser, M. M., Raymond, P. A., and Wickland, K. P.: A decrease in discharge-normalized DOC export by the Yukon River during summer through autumn, Geophys. Res. Lett., 32, L21413, https://doi.org/10.1029/2005GL024413, 2005.

Sun, G., Riekerk, H., and Kornhak, L. V.: Ground-water-table rise after forest harvesting on cypress-pine flatwoods in Florida, Wetlands, 20, 101–112, 2000.

Thivolle-Cazat, A. and Najar, M.: Évolution de la productivité et de la récolte du pin maritime dans le massif Landais. Evaluation de la disponibilité future en Gironde, Revue forestière française, 53, 351–355, 2001.

Thornthwaite, C. W.: An approach toward a rational classification of climate, Geogr. Rev., 38, 55–94, 1948.

Tsypin, M. and Macpherson, G. L.: The effect of precipitation events on inorganic carbon in soil and shallow groundwater, Konza Prairie LTER Site, NE Kansas, USA, Appl. Geochem., 27, 2356–2369, 2012.

Venkiteswaran, J. J., Schiff, S. L., and Wallin, M. B.: Large Carbon Dioxide Fluxes from Headwater Boreal and Sub-Boreal Streams, PLoS ONE, 9, e101756, https://doi.org/10.1371/journal.pone.0101756, 2014.

Vernier, F. and Castro, A.: Critère "Préservation de l'environnement", sous-critère "Eau", Rapport d'expert dans le cadre de l'expertise sur l'avenir du massif forestier des Landes de Gascogne: GIP ECOFOR, Bordeaux, France, 39 pp., 2010.

Vincke, C. and Thiry, Y.: Water table is a relevant source for water uptake by a Scots pine (Pinus sylvestris L.) stand: Evidences from continuous evapotranspiration and water table monitoring, Agr. Forest Meteorol., 148, 1419–1432, 2008.

Vissers, M. J. and van der Perk, M.: The stability of groundwater flow systems in unconfined sandy aquifers in the Netherlands, J. Hydrol., 348, 292–304, 2008.

Wallin, M. B., Grabs, T., Buffam, I., Laudon, H., Ågren, A., Öquist, M. G., and Bishop, K.: Evasion of CO_2 from streams – The dominant component of the carbon export through the aquatic conduit in a boreal landscape, Glob. Change Biol., 19, 785–797, https://doi.org/10.1111/gcb.12083, 2013.

Warren, J. M., Meinzer, F. C., Brooks, J. R., and Domec, J. C.: Vertical stratification of soil water storage and release dynamics in Pacific Northwest coniferous forests, Agr. Forest Meteorol., 130, 39–58, 2005.

Weiss, R.: Carbon dioxide in water and seawater: the solubility of a non-ideal gas, Mar. Chem., 2, 203–215, 1974.

Wilson, H. F., Saiers, J. E., Raymond, P. A., and Sobczak, W. V.: Hydrologic drivers and seasonality of dissolved organic carbon concentration, nitrogen content, bioavailability, and export in a forested New England stream, Ecosystems, 16, 604–616, 2013.

Xu, Y.-J., Burger, J. A., Aust, W. M., Patterson, S. C., Miwa, M., and Preston, D. P.: Changes in surface water table depth and soil physical properties after harvest and establishment of loblolly pine (Pinus taeda L.) in Atlantic coastal plain wetlands of South Carolina, Soil Till. Res., 63, 109–121, 2002.